Final report

Habitat modeling of Atlantic blue marlin with SEAPODYM and satellite tags

Michael J. Schirripa, SEFSC, Sustainable Fisheries Division, Miami FL

Jiangang Luo, University of Miami, Rosenstiel School of Marine and Atmospheric Science, Miami, FL

Patrick Lehodey and Inna Senina, Marine Ecosystem Modelling and Monitoring by Satellites, CLS, Satellite Oceanography Division, 8-10 rue Hermes, 31520 Ramonville, France

Eric Prince, Southeast Fisheries Science Center, Sustainable Fisheries Division, Miami FL

Jay R. Rooker, Department of Marine Biology, Texas A&M University at Galveston
5007 Ave U, Galveston, Texas 77551

Abstract

The variability of Atlantic blue marlin habitats and spatial dynamics was studied through the combined use of a state of the art ecosystem model (SEAPODYM) and movement data from electronic satellite tags. We compiled and analyzed 120 Popup Archival Transmitting (PAT) tags deployed on Atlantic blue marlin from 2002 to 2008 in the Atlantic and the Gulf of Mexico. A preliminary model was parameterized using assimilation of depth, temperature and movement tracks from PAT data and general knowledge on tuna and billfishes. The model was used to estimate the habitat index of the blue marlin. In general, the seasonal patterns of blue marlin habitat from model matched well with the observed data. To test the performance of the model on feeding habitat, we conducted sensitivity analysis by changing the optimal feeding temperatures and the DO threshold levels, and for spawning habitat by changing the optimal surface temperature for juvenile. Habitat indices were analyzed by calculated the area in square kilometer at two levels (0.1 and 0.5). Feeding habitat area decreased as the optimal feeding temperature and DO threshold increased, and the high quality habitat (>0.5) decreased faster than the lower quality habitat (>0.1). Similarly, the spawning habitat area also decreased as the optimal surface temperature for juvenile increased. However these limited tagging data are not informative enough to correctly estimate the movement patterns at the scale of population. Further researches are necessary to continue this work and to move on to the next step of model parameterization, especially the use of fishing data (effort, catch and size) to evaluate the habitat modeling and to improve parameterization of population movements and migrations.

Introduction

Blue marlins (*Makaira nigricans*) are a large apex pelagic predator species within the family of Istiophorida (the billfish). Their growth rate is among the fastest documented for a fish species and can reach weights in excess of one thousand pounds with females growing significantly larger than males (cite). They display extensive movements within and across the Atlantic, as demonstrated from various tagging studies (cite). Spawning takes place over a wide seasonal time range with a peak occurring in the summer months. Little information is available on the larval and juvenile stages as they rarely occur in biological samples (Serafy et al. 2006).

The International Commission for the Conservation of Atlantic Tuna (ICCAT) is responsible for the management of the Atlantic blue marlin. Catches of blue marlin are predominately incidental from surface longline fisheries targeting tuna, however, there are also documented catches from near-shore gillnet fisheries (cite). There is also a substantial targeted recreational fishery in North and South America as well as the Caribbean, with most of the fish being released. The ICCAT manages the Atlantic as a single unit stock. Traditionally the Atlantic blue marlin has been assessed using variations on stock-production models. Generally, this is because very little data on this species has been available and these types of models are often times appropriate for data poor situations. Despite the fact that tuna and billfishes are well known to be distributed in time and space based on oceanographic conditions, none of the above mentioned modeling platforms (and consequently the resulting assessments) explicitly takes into account fish habitats and their variability. The longest observational data set available to assess blue marlin is the Japanese longline catch per unit effort (CPUE) series. This data set begins in 1956 and covers what is believed to be the beginning of any significant fishing mortality on the species. No other data dates this far back, making the Japanese CPUE critical in determining stock status. This index displays a marked decline from 1957 to 1980. Coincident with this decline is the fact that the Japanese fleet gradually shifted their effort and gear configurations from targeting yellowfin tuna to targeting bigeye tuna. It has been hypothesized that this shift in targeting by the Japanese fleet is at least partly responsible for the observed decline in CPUE during the 60's and 70's. "Although making occasional forays down to greater depths and colder water temperatures, yellowfin tuna spend upwards of 90% of the time at depths where the water temperature is no more than 8 degrees C colder than surface layer temperature (Brill. Col. Vol. Sci. Pap. ICCAT, 57(2): 142-161 (2005). Like yellowfin tuna, the marlins do occasionally make forays down to colder water temperatures, but spend upwards of 90% of the time at depths where the water temperature is are within 1° to 2° of the SSTs ((Hinton 2003?, IATTC blue marlin assessment). In contrast, bigeye tuna regularly expose themselves to temperature changes of up 20 degrees C during their daily vertical movements" (Brill. Col. Vol. Sci. Pap. ICCAT, 57(2): 142-161 (2005). While other explanations are possible, the decline in blue marlin CPUE by the Japanese fleet may be due, at least in part, to a change in the fleets blue marlin catchability.

SEAPODYM is a modeling approach that describes spatial population dynamics based on environmental relationships and the definition of species habitat (Lehodey et al. 2008). This model also includes a parameter optimization framework based on likelihood approach (Senina et al., 2008) that has been applied to four Pacific tuna species (Lehodey and Senina 2009, WCPFC) and is used to investigate the impact of climate change on tuna (Lehodey et al 2010). The model is driven by environmental variables (temperature, currents, primary production, and dissolved oxygen concentration) between surface and a depth of 1000 m. Predicted feeding and spawning habitats are used to model the movement of fish based on a system of advection-diffusion equations.

This study is aimed at identifying the main sources of variability of Atlantic blue marlin habitats and spatial dynamics, through the combined use of a state of the art ecosystem model and movement data from electronic tags. The increased availability of recent data on the ocean scale movements for blue marlin using electronic tags (Prince and Goodyear 2006; Goodyear et al. 2008; and Prince et al. 2010) facilitated our species selection process. The emphasis of the first phase of this project was to put on defining the feeding habitat, based on mechanisms developed in the model for other billfish species, in order to recreate the key movement patterns of individuals, as described by archival tags. A review covering biology, ecology, fisheries and population structure of Atlantic blue marlin will be conducted to gather all the necessary information needed to parameterize the model SEAPODYM are to be conducted for the second phase of the study.

The longer term objective of the research was to produce a reliable spatial habitat map for a habitat based stock assessment and compare the biomass and mortality estimates to those coming from the current stock assessment model (Stock Synthesis) that does not consider habitat.

Materials and methods

Wildlife Computers (www.wildlidfecomputers.com, Redmond, WA, USA) electronic tags (popup satellite archival tags, PSATs) were used to monitor horizontal habitat use of blue marlin in the Atlantic and the Gulf of Mexico (Figure 1). In-water tagging techniques and associated equipment described in our previous work (Prince and Goodyear 2006, Prince et al. 2010). The tags were programmed to sample depth (pressure), temperature and light once every 30s. The depth and temperature records for were summarized by the on-board software into histograms at 6-hour bin intervals. We programmed the tag to summarize temperature bins starting at <12°C, then each successive 2°C interval ending with >32°C. Likewise, depth bins started at <-1 m, then successive intervals of 25 m until ending at depths >250 m. Eight profiles of depth and temperature (PDT) were also summarized by the on-board software at 6-hours intervals, which gave minimum and maximum temperatures for the shallowest and deepest depths, and for 6 depths between. Fish movement tracks were derived from light-level,

temperature, and bathymetric data. Light-level geolocation data were initially processed using the global positioning software WC-AMP (Wildlife Computers), and then applying a sea-surface temperature-corrected Kalman filter (Nielsen et al., 2006) to the light-level-derived locations. Finally, we used a custom bathymetry filter to relocate the points that were on land or in shallow water, based on 2 x 2 minute grid ETOP02 bathymetry data (Anon., 2006) and the daily maximum depth from the PSAT (Hoolihan and Luo, 2007). The daily movement tracks were aggregated into 6 days average positions and its 95% confidence interval as inputs for the Seapodym model. We also calculated kernel density for the 6 day aggregated data according to the algorithms by Worton (1995) for comparison to model habitat distribution. Kernel density values are cumulated from the highest to lowest density areas (Worton 1989). Thus, the 25% contours represent areas of the top highest observed densities, while the 95% contours represent up to 95% density areas.

We used SEAPODYM as the main tool for habitat modeling. This model was developed to simulate the spatial dynamics of tuna populations in the pelagic ecosystem. It uses bio-physical environmental fields to simulate the upper trophic levels of marine ecosystem organized in two groups: the blue marlin and its prey species of the mid-trophic levels (i.e. micronekton). Modeling the habitat and vertical structure of micronekton distribution, as well as the age-structured spatial dynamics of blue marlin (through an advection-diffusion framework) is based on first biological principles, such as thermal habitat, oxygen tolerance, prey and predator interactions. The parameterization of these components defines a movement index with seasonal switching between feeding and spawning habitats, defining in turn the spatial dynamics of the target species (Lehodey et al 2010).

The model domain covers the Atlantic Ocean and the Gulf of Mexico with a grid extending from 40 S to 65 N and 100 W to 20 E at 0.25 degree resolution (**Figure 1**). To drive the intermediate trophic functional groups, we used physical and biogeochemical forcing data sets derived from a coupled physical–biogeochemical model (Lehoedey et al 2010). We used the physical reanalysis GLORYS (GLobal Ocean ReanalYsis and Simulations) that was provided by the French Groupe Mission Mercator Coriolis, at a resolution of ¼ deg x 6 days, and using data assimilation to provide higher realistic prediction. We used satellite derived primary production at the same resolution to run a simulation with the micronekton model (Lehodey et al., 2010), for the period 2002-2009.

Results

We have compiled and analyzed 80 Popup Archival Transmitting (PAT) tags deployed on Atlantic blue marlin in the Atlantic from 2002 to 2004, and 43 PAT tags in the Gulf of Mexico from 2003 to 2008. Of the 80 Atlantic tags, 46 tags were determined to contain useful data, and 39 of the Gulf of Mexico tags have good data. The 6 day aggregated track locations and their 95% confidence intervals for all tags are shown in **Figure 1**. We have also compiled the

conventional tagging data base to analyze the distribution of conventionally tagged Atlantic blue marlin **(Figure 2**). Depth distribution and temperature distribution of PAT tag data were also analyzed (**Figure 3, 4**). The statistics of the temperatures and depths were summarized in **Table 1**. The mean temperatures for all tags were 27.59 ^{o}C, 28.22 ^{o}C, and 28.6 ^{o}C for day, twilight and night. The overall mean temperature was 27.98 ^{o}C. The mean depths for all tags were 53.6 m, 33.0 m and 22.2 m for day, twilight and night.

Table 1. Statistics of temperatures and depths from PAT tags

	Temperature ^{o}C			Depth (m)	
	Mean (stdev)	Max	min	Mean (stdev)	Max
Day	27.59 (1.98)	32	9.15	53.6 (50.4)	787
Twilight	28.22 (1.64)	32	12.06	33.0 (38.6)	516
Night	28.60 (1.05)	32	18.12	22.2 (25.9)	275
Overall	27.98 (1.70)	32	9.15	40.0 (44.8)	787

Blue marlin kernel density distributions were estimated quarterly based on 6 day aggregated PAT tag track positions (**Figure 5**). For January to March, most track locations were in the Gulf of Mexico with, and the core kernel (0-25%) is located in southern part of the gulf. For April to June, we have track locations in the Gulf of Mexico, around Bahamas, and east Atlantic, but the core kernel estimate is located in northern Gulf of Mexico and Bahamas. From July to September, it has similar kernel distributions as the last quarter but more spread out to the Antilles. In the last quarter, 50% kernel spread out to most of the Gulf of Mexico, and in the Atlantic the core kernel (0-25%) is located around Porto Rico with 95% kerned extended to the mouth of the Amazon River.

The distribution of blue marlin feeding habitat from Seapodym model simulation runs are shown in **Figure 6** to **Figure 13,** and are summarized in **Table 2**. In general, feeding habitat areas decreased as the optimal feeding temperature (T_a) increased (**Figure 14**) at both high quality habitat (>0.5) and low quality habitat (0.1) levels. Also, there were seasonal differences in feeding habitat areas for both habitat quality levels with smaller areas in first two quarters and greater areas in later two quarters. The patterns of feeding habitat were very similar for the four optimal feeding temperature simulations at the DO threshold $\hat{O}$=4.5 ml/L (**Figure 6, 7, 8,** and **9**). In the first quarter, the core feeding habitat (orange and red color in **Figure 6**) was located around the Antilles. In the second quarter, the core feeding habitat extended to the east to the mid-Atlantic ridge. In the third quarter, the core feeding habitats spread to east tropical east Atlantic, the Gulf of Mexico, and north Atlantic along the path of the Gulf Stream. In the last quarter, the core habitat retreated back to the Antilles in west Atlantic but in the east Atlantic the core habitat area enlarged for the T_a=26.5 simulation (**Figure 6**). Feeding habitat areas also decreased as the DO threshold level increased (**Figure 10**, **11**, **12**, **13** and **15**) at both high quality habitat and low quality habitat levels. However, the changes were much dramatic (average of 10 folds change) at high quality level (**Figure 15A**) than the changes (average of less than 1 fold) at the low quality level (**Figure 15B**).

Table 2. Areas (in 1000 km^2) of quarterly averaged habitat indices at two levels (>0.5 and >0.1) from Seapodym model simulation runs. T_a is the optimal feeding temperature (^oC), Ô is the DO threshold (ml/L), T_o is the optimal surface temperature for larval fish, and q1 to q4 indicate the quarters of the year.

Feeding	Parameters		Feeding Habitat index >0.5				Feeding Habitat index >0.1			
habitat	T_a	Ô	q1	q2	q3	q4	q1	q2	q3	q4
Figure 6	26.5	4.5	152	307	1096	1284	27675	27432	31951	32231
Figure 7	27.5	4.5	80	238	643	183	19983	20908	26701	26000
Figure 8	28.5	4.5	35	108	314	134	13240	13800	19880	18351
Figure 9	29.5	4.5	14	35	56	68	6810	8378	12259	11513
Figure 10	27.5	4.0	513	1346	2097	1753	24345	24496	28936	29548
Figure 11	27.5	3.5	2226	3318	4152	4109	27141	26618	30522	32040
Figure 12	27.5	3.0	3056	4249	5391	5290	28283	27730	31485	33611
Figure 13	27.5	2.5	3400	4545	5858	5789	28661	28228	32086	34116
Spawning Habitat	T_o		Spawning habitat index >0.5				Spawning habitat index >0.1			
Figure 16	27.25	NA	1396	2237	1715	1277	9836	11907	13070	13655
Figure 17	27.75	NA	582	1474	1269	973	7273	9167	10485	10857
Figure 18	28.25	NA	319	678	995	627	4283	6792	8130	8408
Figure 19	28.75	NA	229	348	658	396	1426	3754	5549	5416

In Seapodym model, spawning habitat index is a function of surface layer temperature, micronekton biomass in the surface layer and primary production converted to the wet weight of zooplankton. We made simulation runs on four optimal surface layer temperatures (T_0 = 27.25, 27.75, 28.25 and 28.75 ^oC) for juvenile blue marlin (**Figure 16** and **19**). The results were also summarized in **Table 2.** Similar to feeding habitat index, the spawning habitat areas decreased as the optimal surface layer temperature (T_0) for juvenile increased (**Table 2, Figure 20**) at both high quality habitat (>0.5) and low quality habitat (0.1) levels. The pattern of blue marlin spawning habitat distribution is mostly limited from Florida to the east tip of South America in Brazil (**Figure 16, 17, 18, 19**) with small variations. In the first quarter, the spawning habitat is limited to the south of Florida. In the second quarter, it extends into the Gulf of Mexico and the Bahamas. In the summer (third quarter), it extends further to southeast coast of the USA, north Atlantic along the path of the Gulf Stream, and around the Bermuda. In the fall (fourth quarter), the spawning habitat is limited to the south of Cape Hatteras, USA.

Most of PAT tag locations were located inside the feeding habitat level >0.1 areas, especially for the third (76 to 98%) and fourth (38 to 99 %) quarters among all simulation runs (**Table 3**). At an intermediate habitat quality level (>0.3), the percent overlaps were still over 50% for about half of the simulations runs. However, only small percentages (0 to 39%) of tag locations were overlapped with the high habitat quality level (>0.5). The spawning habitat index had much less overlap (last two rows in **Table 3**) with tag locations compared with feeding habitat.

Table 3. -Overlap of PAT tag locations with three levels (>0.1, >0.3, >0.5) of habitat quality. T_a is the optimal feeding temperature (^oC), Ô is the DO threshold (ml/L), T_o is the optimal surface temperature for larval fish, and q1 to q4 indicate the quarters of the year. The values are the percent of locations inside each habitat quality areas.

Feeding	Parameters		Feeding Habitat index >0.5				Feeding Habitat index >0.3				Feeding Habitat index >0.1			
Habitat	T_a	Ô	q1	q2	q3	q4	q1	q2	q3	q4	q1	q2	q3	q4
Figure 6	26.5	4.5	0.0	1.0	13.3	2.2	10.6	9.3	64.4	25.1	85.1	91.2	97.2	90.1
Figure 7	27.5	4.5	0.0	0.5	5.1	1.3	2.1	3.6	45.1	9.9	44.7	73.1	95.4	81.2
Figure 8	28.5	4.5	0.0	0.0	1.6	1.3	0.0	2.1	15.0	4.9	25.5	23.3	89.9	66.8
Figure 9	29.5	4.5	0.0	0.0	0.2	0.9	0.0	0.5	5.5	1.8	8.5	7.8	76.0	38.1
Figure 10	27.5	4.0	0.0	1.0	17.8	5.4	10.6	7.3	74.1	42.6	70.2	81.9	97.2	92.4
Figure 11	27.5	3.5	2.1	5.2	29.7	10.3	21.3	9.3	82.4	64.6	70.2	89.1	97.8	97.8
Figure 12	27.5	3.0	4.3	5.2	37.0	13.0	25.5	11.4	84.4	71.3	72.3	91.2	97.8	98.7
Figure 13	27.5	2.5	4.3	5.2	38.8	13.5	25.5	13.0	85.0	75.3	72.3	92.7	98.0	99.1
Spawning Habitat	T_o		Spawning habitat index >0.5				Spawning habitat index >0.3				Spawning habitat index >0.1			
Figure 16	27.25	NA	6.4	0.0	2.8	0.0	14.9	0.0	26.1	2.7	29.8	2.6	53.5	9.9
Figure 17	27.75	NA	2.1	0.0	2.8	3.1	6.4	4.1	21.0	25.1	10.6	16.1	46.3	37.2
Figure 18	28.25	NA	0.0	0.0	2.6	0.4	2.1	0.0	11.5	0.4	6.4	0.5	35.2	3.6
Figure 19	28.75	NA	0.0	0.0	1.6	0.4	0.0	0.0	5.7	0.4	4.3	0.0	21.6	1.3

Since our PAT tag data is very limited, we also analyzed the ICCAT longline fishing fleet bycatch data on the blue marlin. We plotted the total blue marlin bycatch by all countries over the map of dissolved oxygen (DO) concentration at 100 m depth (from World Ocean Atlas 2005, **Figure 21**). The large blue marlin bycatch are in the east Caribbean Sea and the coast of central Africa. The intermediate bycatch are mostly inside the 3.5 ml/L DO contour line (defined as oxygen minimum zone, OMZ). However, the large blue marlin bycatches are not necessary indication for the abundances of blue marlin rather the results of heavy fishing efforts towards targeted species (such as tuna, and swordfish) in those areas (**Figure 22**). Since not all countries reported fishing efforts, it is not possible to estimate an accurate CPUE for the total bycatch, but a rather approximate CPUE. This approximate CPUE (**Figure 23**) clearly indicates that the east Caribbean Sea and the water around the Antilles Islands are the best blue marlin habitat which corresponding exactly the same pattern from Seapodym model outs.

There is an alternative to get a more accurate estimate of CPUE, which is to use data from the country that has the best records in both catches and efforts. The Japanese longline fishing fleet had good coverage for the tropical Atlantic. Thus, it should give good estimates of CPUE for the OMZ and the surrounding areas. The seasonal Japanese longline blue marlin CPUE (**Figure 24**) distribution resembles well with the seasonal blue marlin feeding habitat simulated with 2.5 ml/L DO threshold (**Figure 13**) around OMZ.

Discussions

The results of Atlantic blue marlin habitat from Seapodym model simulations are generally matched well with the blue marlin track locations from PAT tagging studies and with the distribution patterns of longline fishing fleet CPUE in the Atlantic. All results indicate that the best blue marlin feeding habitats are located in southern Caribbean Sea, around the islands of Antilles, and the nearby waters east of the Less Antilles. However, there are some high CPUE areas in the OMZ where model simulations indicated low habitat quality. This discrepancy is mostly due to two factors. First, the high blue marlin bycatch CPUEs in the OMZ are not necessary indication of high abundance of blue marlin because inside the OMZ the habitat is vertically compressed by the low DO concentration, which made the longline fishing gears more effective in catching the blue marlin in the narrow surface water which results in relatively higher CPUEs (Prince and Goodyear 2006, 2007; Prince et al 2010; Stramma et al 2011). Thus, if one uses blue marlin bycatch CPUEs as an indicator of habitat quality in that area, it will be over representing the quality of that habitat and thus estimates of abundance. Second, the feeding habitat index from Seapodym model simulation is a vertically integrated habitat index and it assumes that blue marlin move through the water column the same way as they do outside the OMZ. In reality, blue marlin inside the OMZ can only exist in the compressed surface layer (**Figure 3**) of the feeding habitat because most of its prey species inside the OMZ were also compressed to the surface layer. Therefore, the Seapodym model simulations were underestimating the feeding habitat quality inside the OMZ.

The data from our PAT tagging studies played a critical role in parameterizing the model. They provided detailed temperature information on the optimal feeding temperature, vertical distribution data for vertical movement in the model, and horizontal track positions for model calibration. The track position and feeding habitat overlap results (Table 3) show that, depending on simulation scenarios and seasons, as much as 99% of blue marlin track positions are found within the positive (>0.1) feeding habitat, suggesting that the model is performing well. However, one of the short fall of the PAT tag data is that they are mostly in northwestern Atlantic and the Gulf of Mexico and only a few in the east and south Atlantic (**Figure 1**), which made us less confident about the results in those areas. Thus, it is clear that we need to conduct more PAT tagging studies in those areas in the next phase of the research.

The Seapodym model simulation results illustrate the relationship between change of DO threshold and blue marlin feeding habitat areas (**Figure 15**). There is a clear inverse relationship between DO threshold and size of available habitat, with lower thresholds resulting in larger feeding habitat areas (**Figure 15).** This result is very important because the high performance physiology of blue marlin results in high oxygen demands and does not allow this species to adapt to low ambient levels DO. Given that this species cannot tolerate low ambient levels of DO, if the OMZs are expanding due to global warming, feeding habitat areas for this species will be reduced. This trend is confirmed in a number of recent papers using empirical data on

electronic tagging of blue marlin habitat use and DO levels in the ETA and WNA study areas (Prince and Goodyear 2006; Prince and Goodyear 2007; Prince *et. al*. 2010; & Stramma *et al.* 2011). The most recent paper provides an estimated loss of the surface mixed layer habitat, over the last 50 years, totaling about 15% (Stramma *et al.* 2011).

Because differential habitat preference effectively increases fish concentrations within the preferred areas, the rate at which fish are caught as a result of one unit of effort will be different for the same gear when it is fished in less preferred habitat. In other words, blue marlin preferred habitat will have a higher density of blue marlin per cubic meter of water than will less preferred habitat. Consequently, at an equivalent level of overall stock abundance, the CPUE in the preferred habitat will be higher than that of the less preferred habitat simply due to the differences in sampled density. This, in turn, presents implications when using catch per unit effort as an index of relative abundance. If data from the two habitat types are inappropriately combined into one estimate of CPUE for the entire area, it will lead to an inaccurate estimate of abundance and catchability and, subsequently, inaccurate historic estimations of the index of relative abundance of the stock. Furthermore, the resulting index of relative abundance would be even more inaccurate if the preferred habitats were to either expand or contract over time. However, if the CPUE data is partitioned into multiple habitat types and a separate catchability can be reasonably assumed or estimated for each, the inaccuracy can be minimized. This suggests that CPUE standardization of data from the same fishery ⁄ gear ⁄ target from within highly preferred habitat and less preferred habitat should be handled separately.

If the assessment model structure can replicate the spatial structure of the habitats, then separate or spatially interpreted indices can and should be applied to each area ⁄ habitat. There are already several assessment models that include specific spatial structure (catch statistical models such as CASAL, Stock Synthesis, Multifan-CL; and Age structure models like VPA2BOX) and others that attempt direct incorporation of the habitat environmental conditions (e.g., STATHBS). However, the main limitation of these applications is usually the transfer of fish between areas within the temporal stratification, although tagging experiments can provide information to infer movement rates.

Alternatively, differential habitat issues can be addressed directly in the standardization of catch rates. In principle, the calculation of CPUE could be stratified spatially for habitats with similar preference classifications. One possible approach would be to classify each of the ICCAT statistical grids into one of several categorical variables, with each category denoting varying degrees of habitat preference. Grid assignments could be based directly on the SEAPODYM output for that particular grid and then a "grid effect" as a categorical variable could then be used in a GLM standardization with the model statement explicitly accounting for the habitat preference category. In a similar manner, the habitat preference output from SEAPODYM could be used a continuous variable in the GLM standardization. In this approach, the habitat preference for each ICCAT grids could be standardized to a maximum of one (denoting the highest preference) and each grid assigned a value from 0-1 based on its particular

preference rating. As we have shown that the habitat preference rating for any particular grid changes with season, an interaction term would likely be advisable.

The SEAPODYM model output could also be used as an aid in the design of time-area closures as a means to reduce fishing mortality. By targeting the closure in the areas of the highest habitat preference the closures could be designed to minimize interactions with fishing gear within time and space. Although this could also be done by merely examining the spatial characteristics of the catch (i.e. bycatch) data, using current habitat data would allow for a more "real time" approach to where gear should be set to best avoid interactions with blue marlin given the current oceanographic conditions.

References:

Anon (2006) US Department of Commerce, National Oceanic and Atmospheric Administration, National Geophysical Data Center. 2-minute Gridded Global Relief Data (ETOPO2v2). http://www.ngdc.noaa.gov/mgg/fliers/06mgg01.html.

Goodyear, C Phillip; Luo, Jiangang; Prince, Eric D; Hoolihan, John P; Snodgrass, Derke; Orbesen, Eric S; Serafy, Joseph E. (2008). Vertical habitat use of Atlantic *blue marlin* Makaira nigricans: interaction with pelagic longline gear. Marine Ecology Progress Series [Mar. Ecol. Prog. Ser.]. Vol. 365, pp. 233-245. 2008.

Hoolihan, J.P. and Luo, J. 2007. Determining summer residence status and vertical habitat use of sailfish (Istiophorus platypterus) in the Arabian Gulf. ICES J. Mar. Sci. 64:1791–1799.

Lehodey, P., Senina, I., Murtugudde, R., 2008. A spatial ecosystem and population dynamics model (SEAPODYM) – Modeling of tuna and tuna-like populations. *Progress in Oceanography* 78 (4), 304-318.

Lehodey P., Murtugudde R., Senina I. (2010). Bridging the gap from ocean models to population dynamics of large marine predators: a model of mid-trophic functional groups. *Progress in Oceanography*, 84: 69–84

Lehodey P., Senina I., Sibert J., Bopp L, Calmettes B., Hampton J., Murtugudde R. (2010). Preliminary forecasts of population trends for Pacific bigeye tuna under the A2 IPCC scenario. *Progress in Oceanography.* 86: 302–315

Lehodey P., Senina I., (2009). An update of recent developments and applications of the SEAPODYM model. Fifth regular session of the Scientific Committee of the Western and Central Pacific Fisheries Commission, 10–21 August 2009, Port Vila, Vanuatu, WCPFC-SC5-2009/EB-WP-10, 44 pp. http://www.wcpfc.int/meetings/2009/5th-regular-session-scientific-committee

Methot, R. D. 2009. Stock assessment: operational models in support of fisheries management. In: The Future of Fishery Science in North America, pp. 137–165. Ed. by R. J. Beamish, and B. J. Rothschild. Fish and Fisheries Series, 31. 736 pp

Nielsen, A., Bigelow, K.A., Musyl, M.K. and Sibert, J.R. 2006. Improving light-based geolocation by including sea surface temperature. Fish. Oceanogr. 15:314–325.

Prince, E. D., and C. P. Goodyear. 2006. Hypoxia-based habitat compression of tropical pelagic fishes. *Fisheries Oceanography.* 15(6): 451-464.

Prince, E. D., and C. P. Gooyear. 2007. Consequencies of ocean scale hypoxia constrained habitat for tropical pelagic fishes. Gulf and Caribbean. Research, 19(2): 17-20.

Prince, E. D., J. Lou, C. P. Goodyear, J. P. Hoolihan, D. Snodgrass, E. S. Orbesen, J. E. Serafy, M. Ortiz, and M. J. Schirripa. 2010. Ocean scale hypoxia-based habitat compression of Atlantic istiophorid billfishes. *Fisheries Oceanography.* 19:448-462.

Senina, I., Sibert, J., Lehodey, P., 2008. Parameter estimation for basin-scale ecosystem-linked population models of large pelagic predators: application to skipjack tuna. *Progress in Oceanography* 78 (4), 319–335

Stramma, L., Prince, E. D., Schmidtko, S., Luo, J., Hoolihan, J. P., Visbeck, M., Wallace, D. W. R., et al. (2011). Expansion of oxygen minimum zones may reduce available habitat for tropical pelagic fishes. *Nature Climate Change*, *2*(1), 33-37. Nature Publishing Group. doi:10.1038/nclimate1304

Figure 1. Six day aggregated blue marlin location (red dots) and 95% confidence ellipses (light grey ellipse) based on PAT tag data.

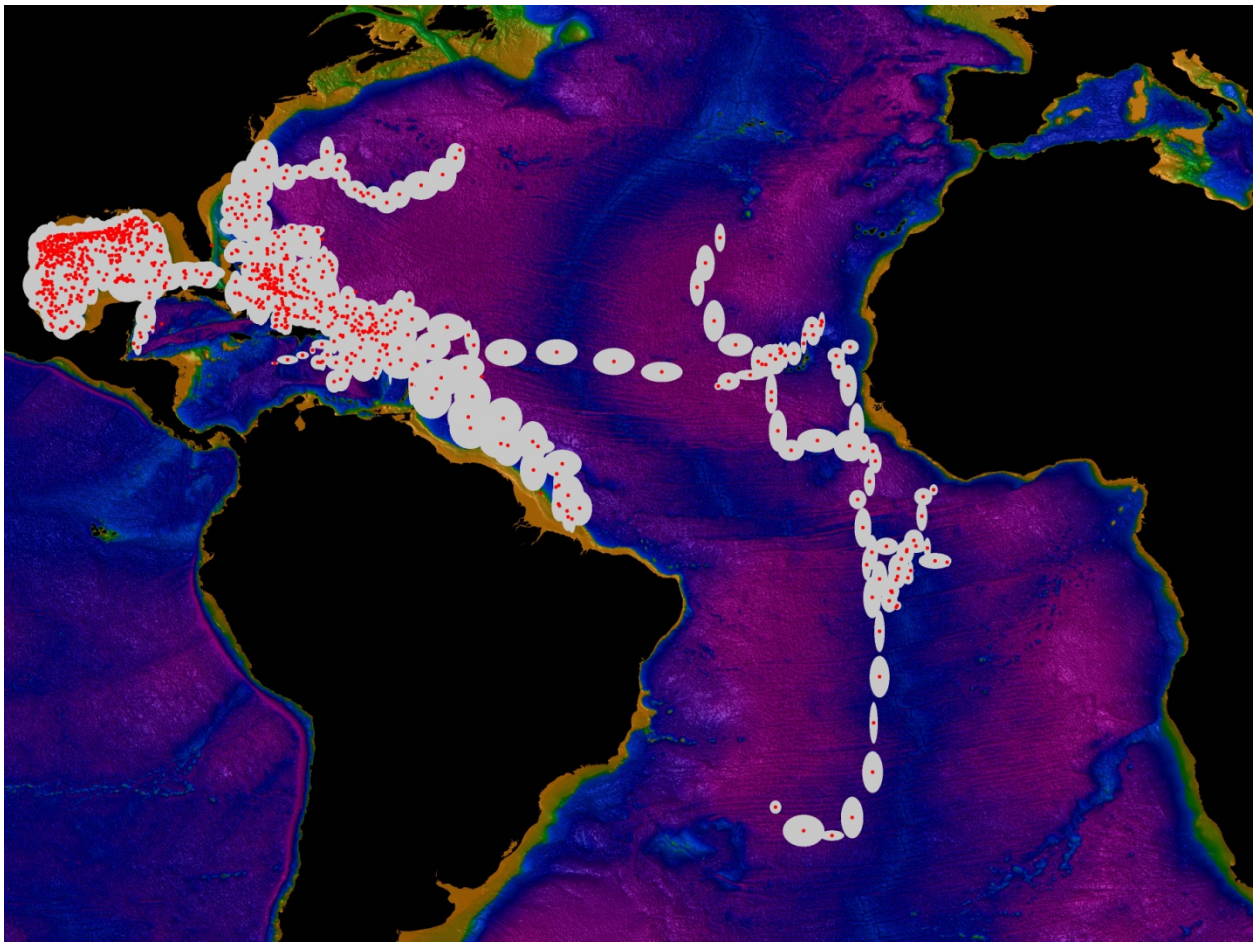

Figure 2. Release locations of conventionally tagged Atlantic blue marlin.

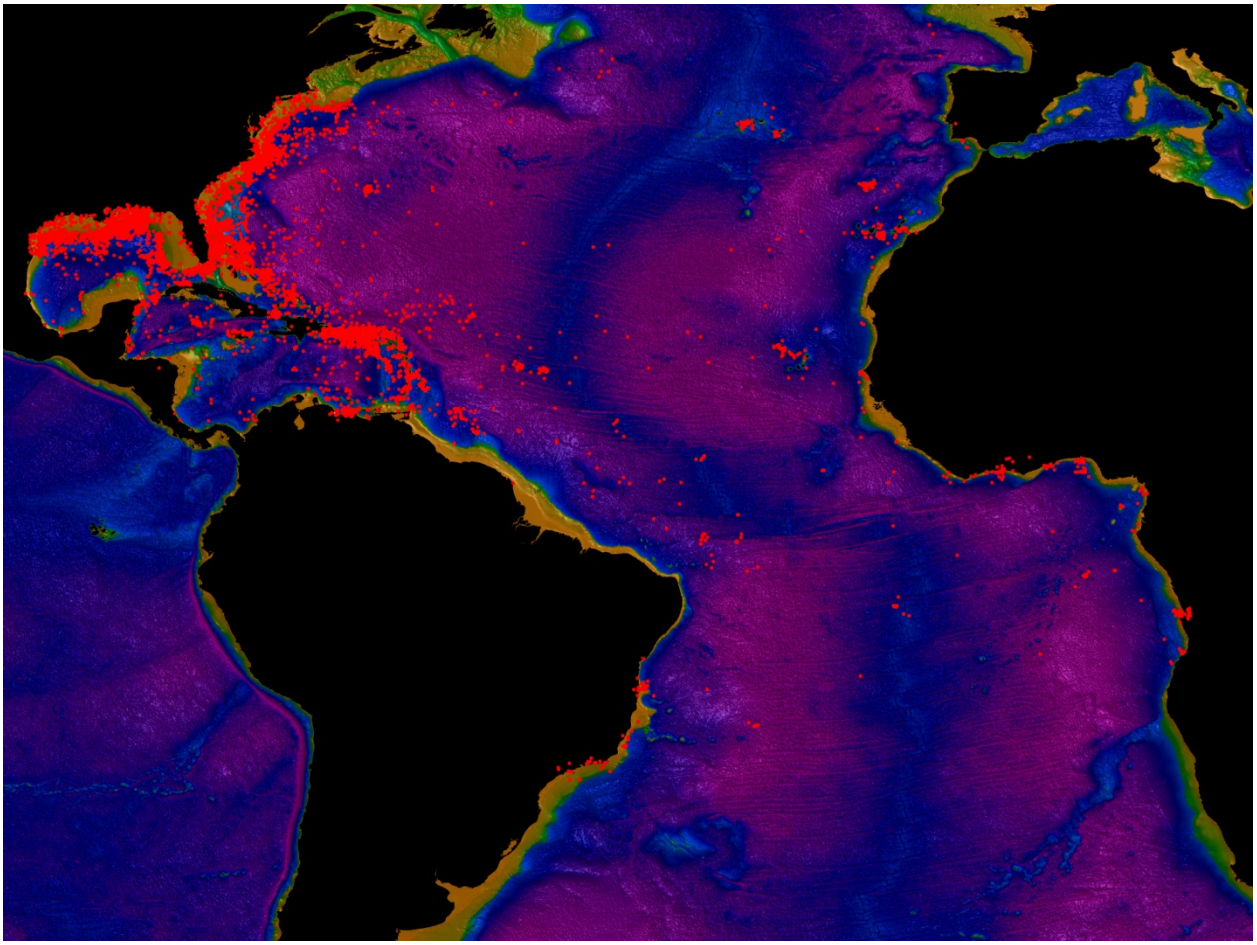

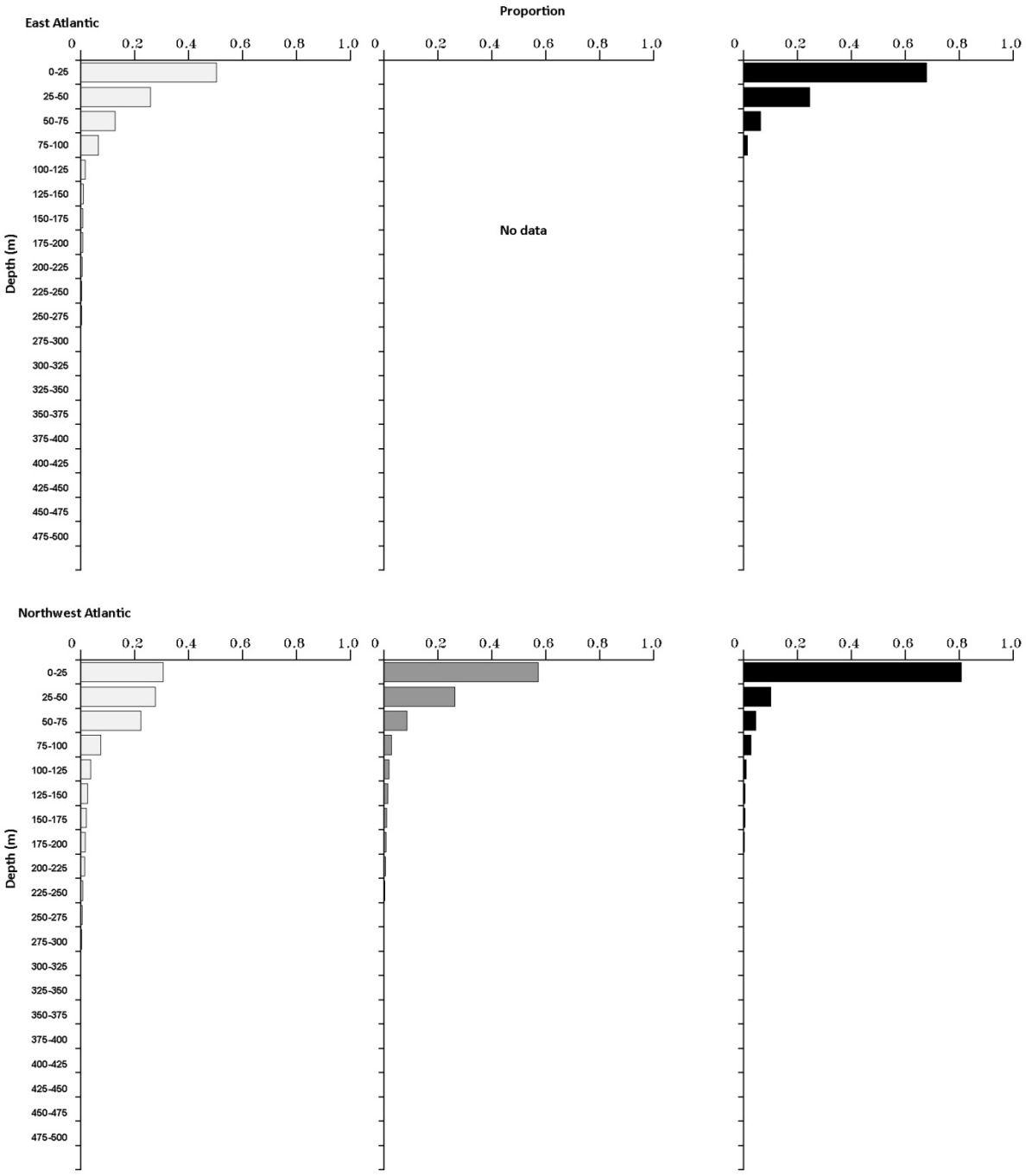

Figure 3. Depth distribution histogram of Atlantic blue marlin by day (light bar), twilight (grey bar), and night (dark bar) for East Atlantic (upper panels) and Northwest Atlantic based on data from PAT tags.

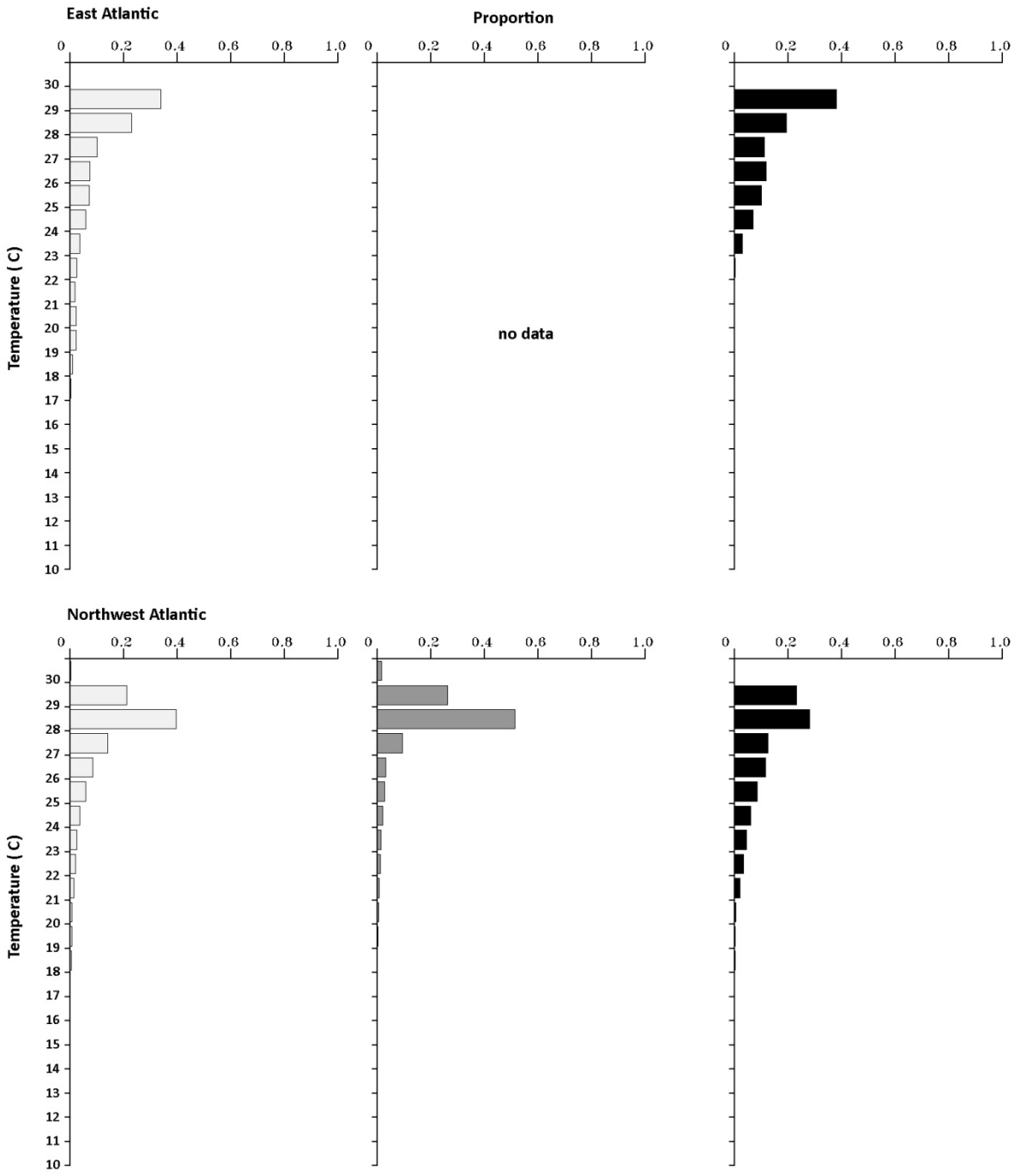

Figure 4. Temperature distribution histogram of Atlantic blue marlin by day (light bar), twilight (grey bar), and night (dark bar) for East Atlantic (upper panels) and Northwest Atlantic based on data from PAT tags.

Figure 5. Quarterly kernel estimate of blue marlin distributions based satellite tag data.

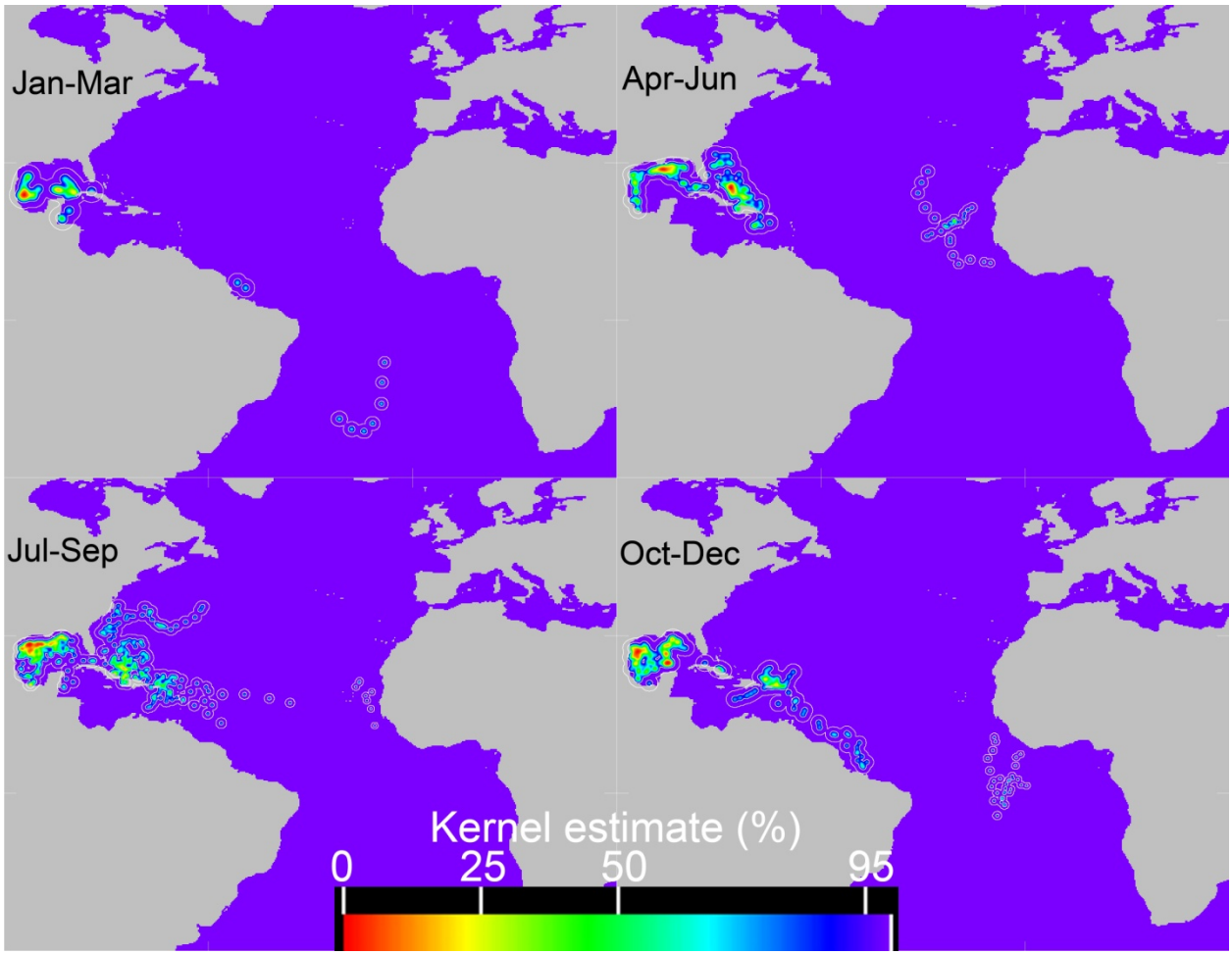

Figure 6. Seasonal average distribution of blue marlin feeding habitats from SEAPODYM model simulation of optimal feeding temperature T_a= 26.5 ^{o}C and DO threshold $\hat{O}$ =4.5 ml/L, over imposed with corresponding tag positions (black +).

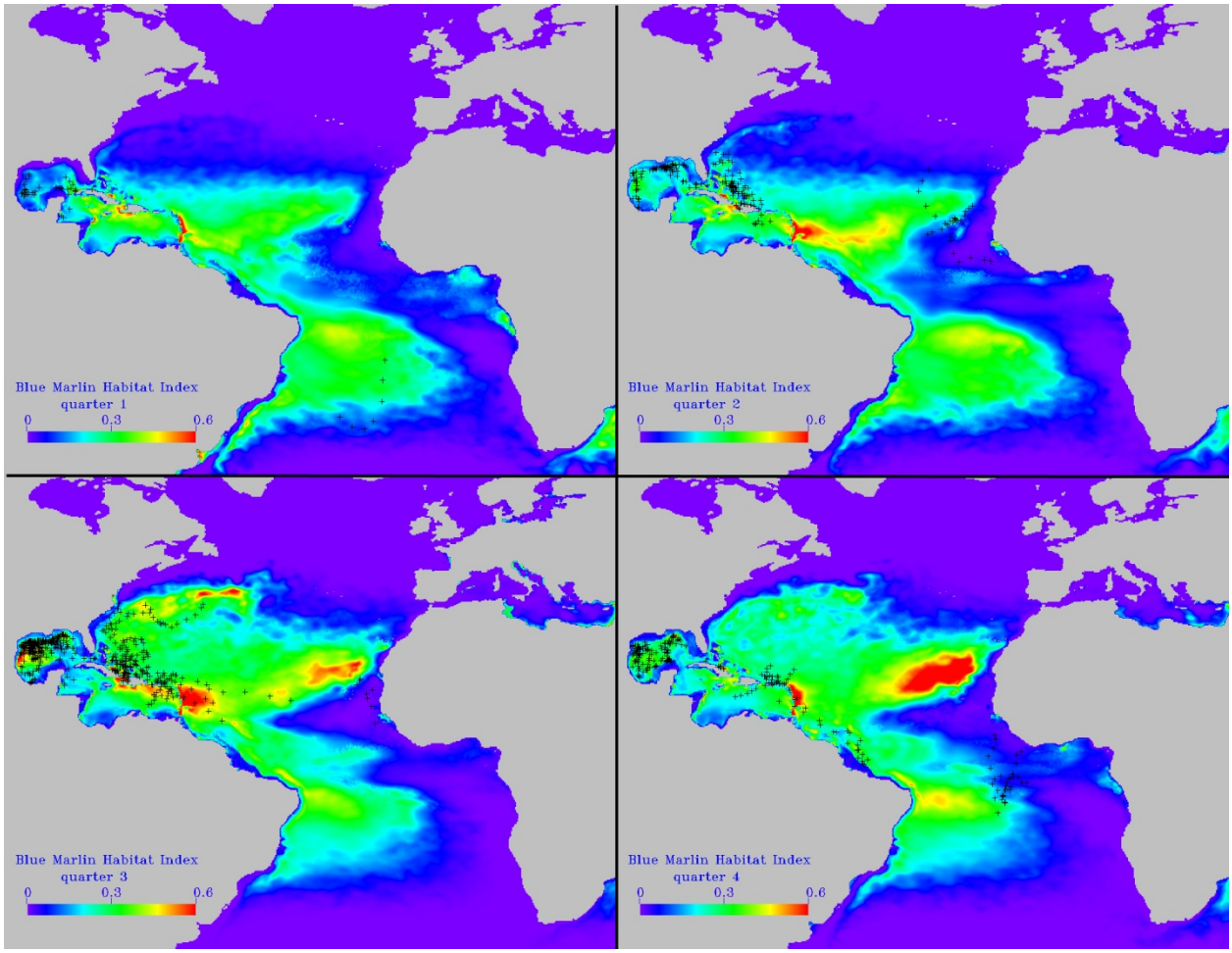

Figure 7. Seasonal average distribution of blue marlin feeding habitats from SEAPODYM model simulation of optimal feeding temperature T_a= 27.5 ^{o}C and DO threshold $\hat{O}$ =4.5 ml/L, over imposed with corresponding tag positions (black +).

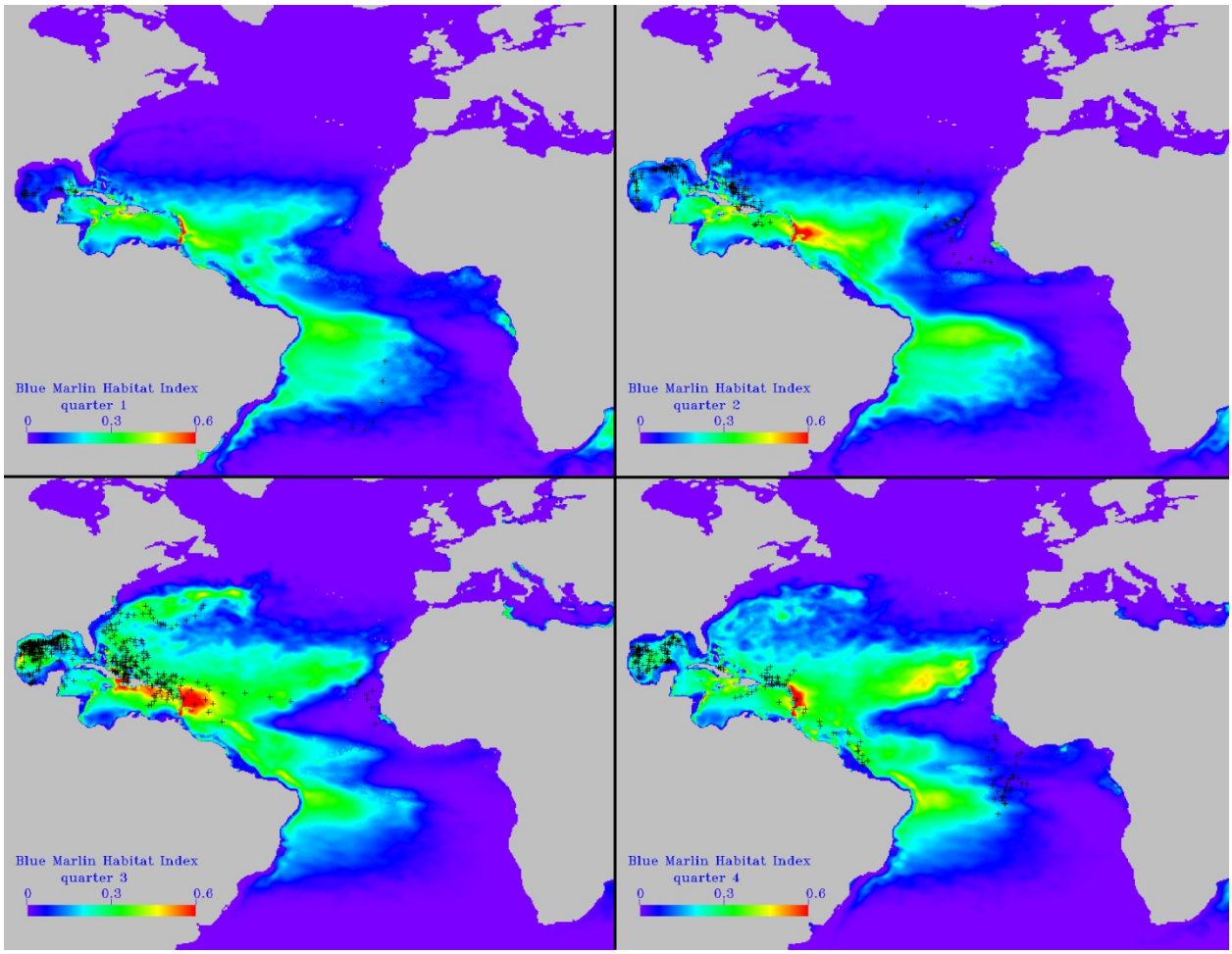

Figure 8. Seasonal average distribution of blue marlin feeding habitats from SEAPODYM model simulation of optimal feeding temperature T_a= 28.5 ^{o}C and DO threshold $\hat{O}$ =4.5 ml/L, over imposed with corresponding tag positions (black +).

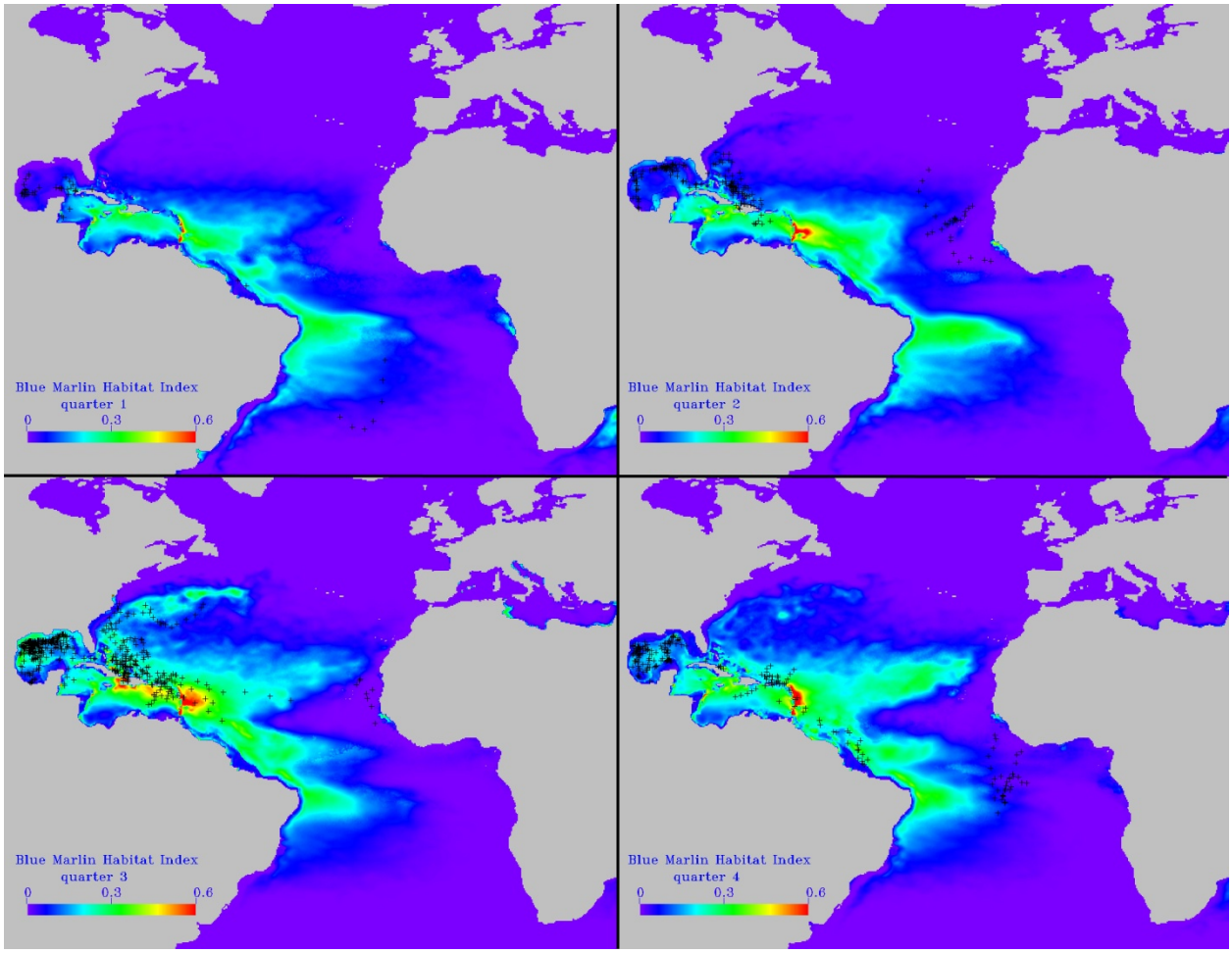

Figure 9. Seasonal average distribution of blue marlin feeding habitats from SEAPODYM model simulation of optimal feeding temperature T_a= 29.5 ^{o}C and DO threshold $\hat{O}$ =4.5 ml/L, over imposed with corresponding tag positions (black +).

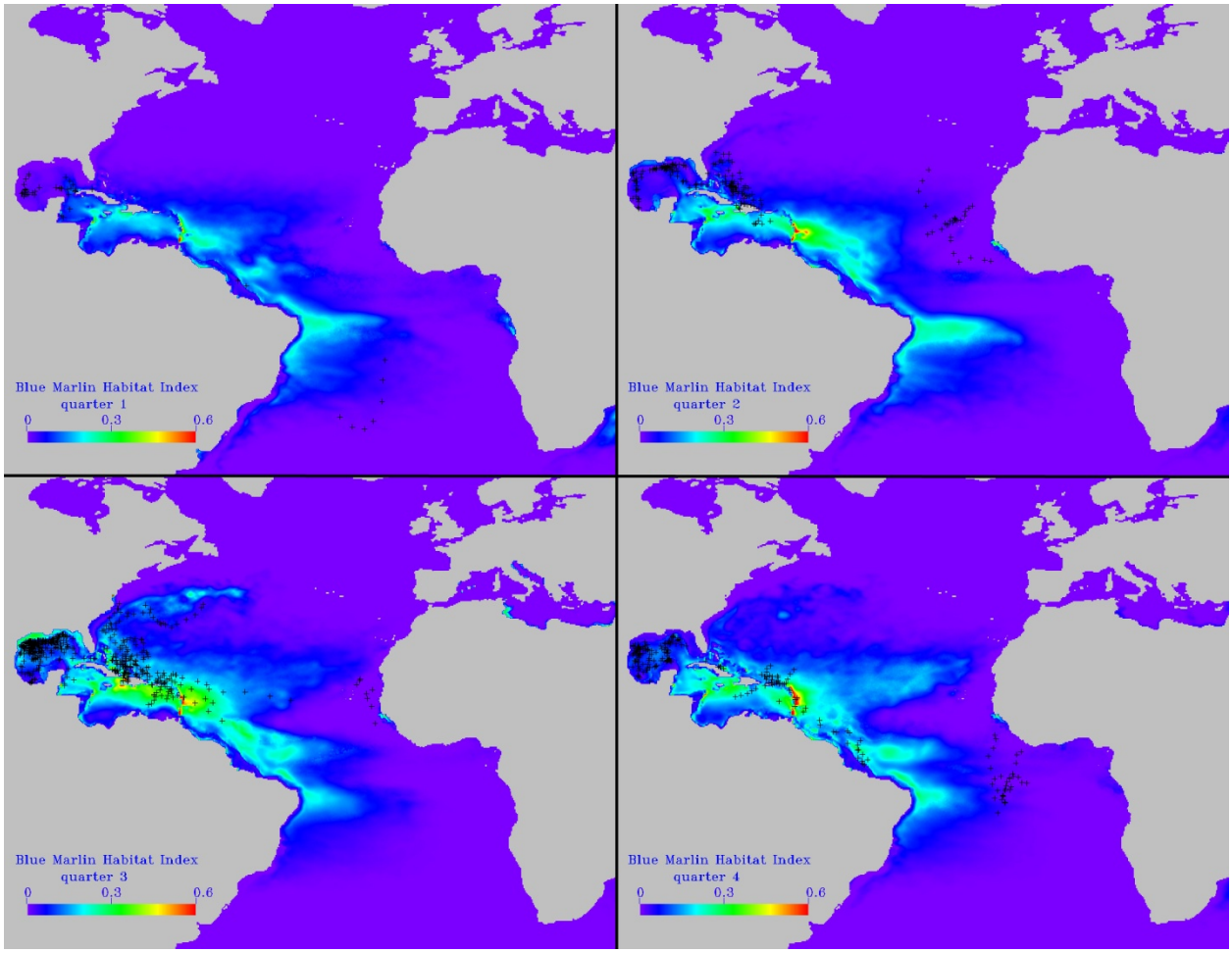

Figure 10. Seasonal average distribution of blue marlin feeding habitats from SEAPODYM model simulation of optimal feeding temperature T_a= 27.5 ^{o}C and DO threshold $\hat{O}$=4.0 ml/L, over imposed with corresponding tag positions (black +).

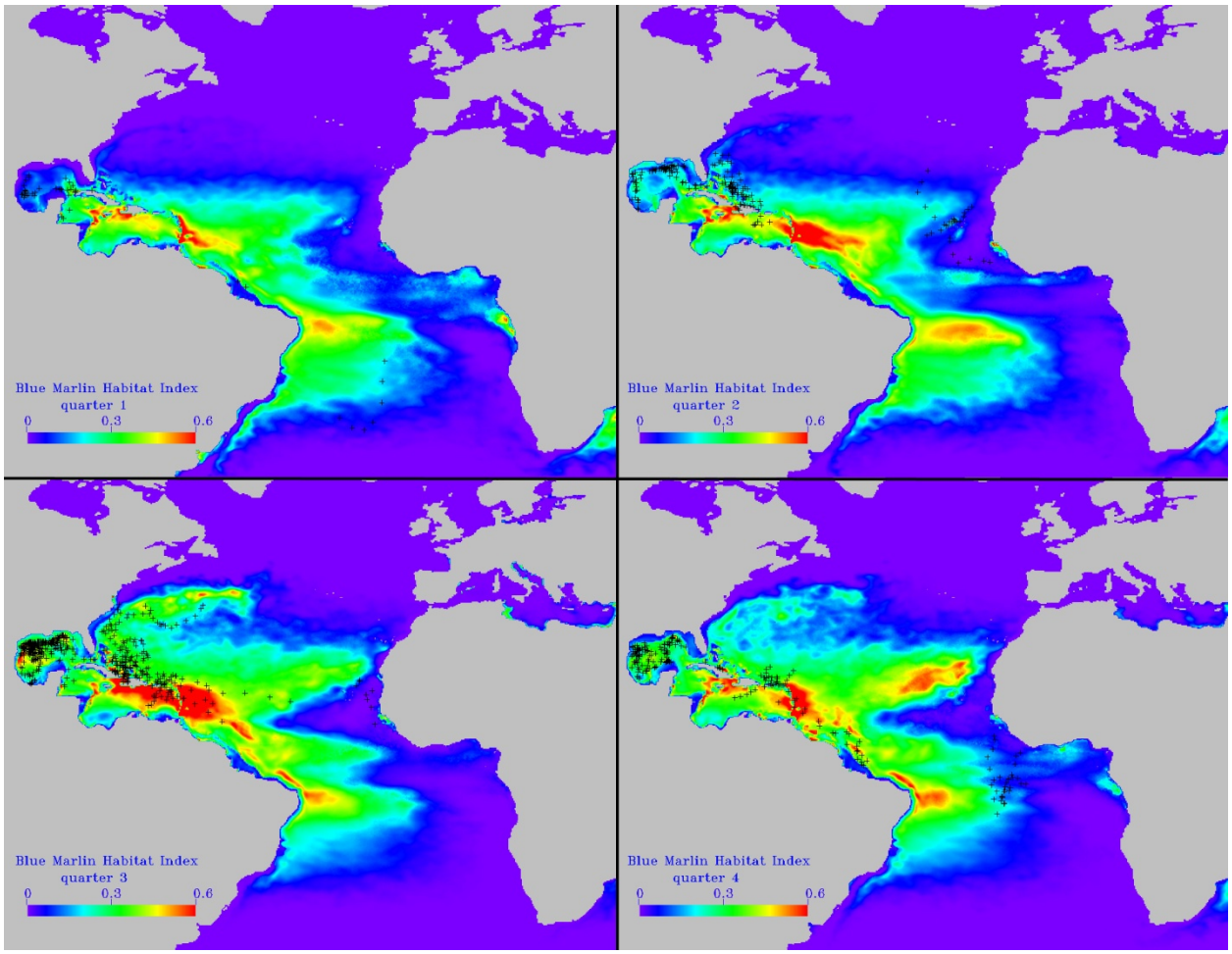

Figure 11. Seasonal average distribution of blue marlin feeding habitats from SEAPODYM model simulation of optimal feeding temperature T_a= 27.5 ^{o}C and DO threshold $\hat{O}$=3.5 ml/L, over imposed with corresponding tag positions (black +).

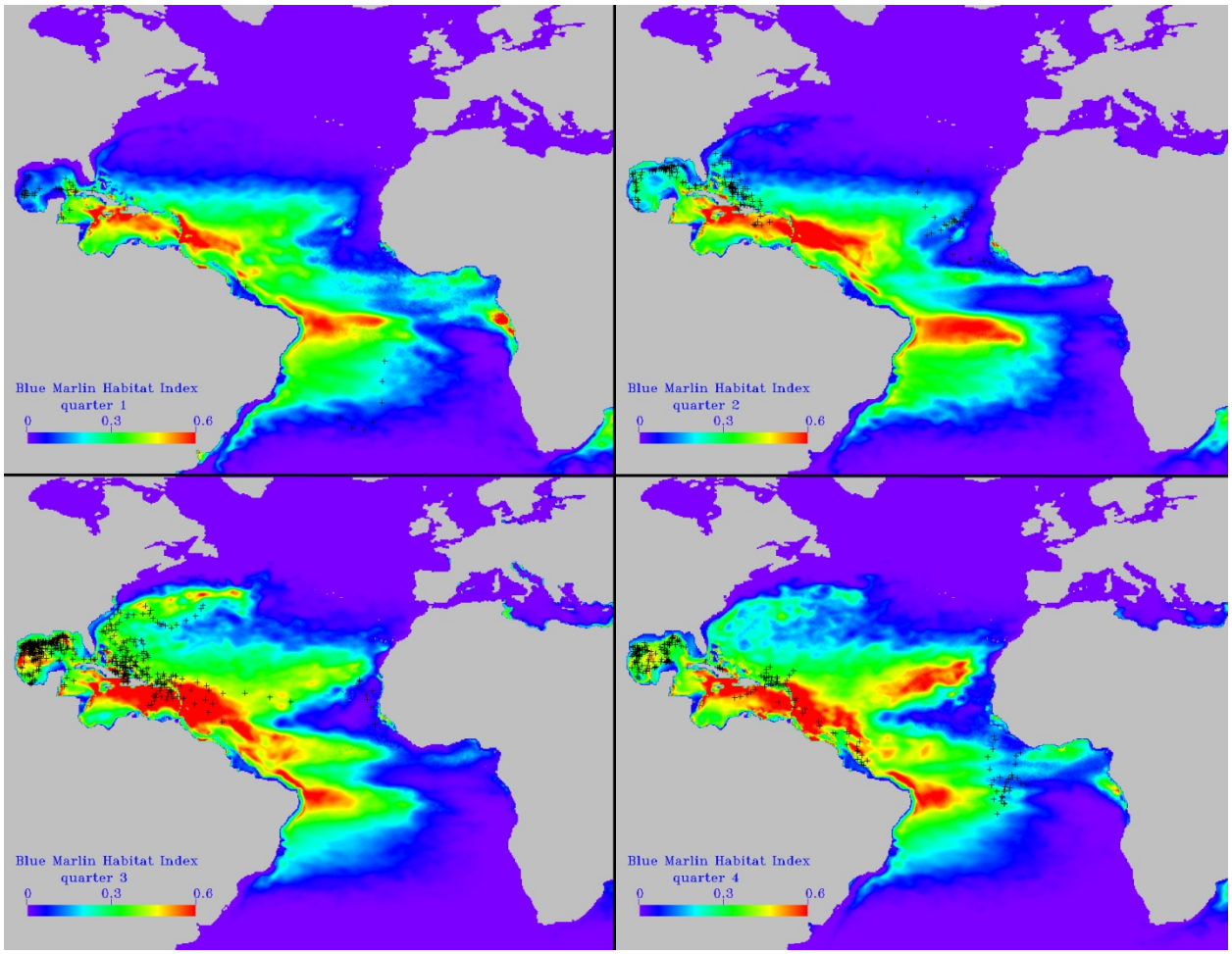

Figure 12. Seasonal average distribution of blue marlin feeding habitats from SEAPODYM model simulation of optimal feeding temperature T_a= 27.5 ^{o}C and DO threshold $\hat{O}$=3.0 ml/L, over imposed with corresponding tag positions (black +).

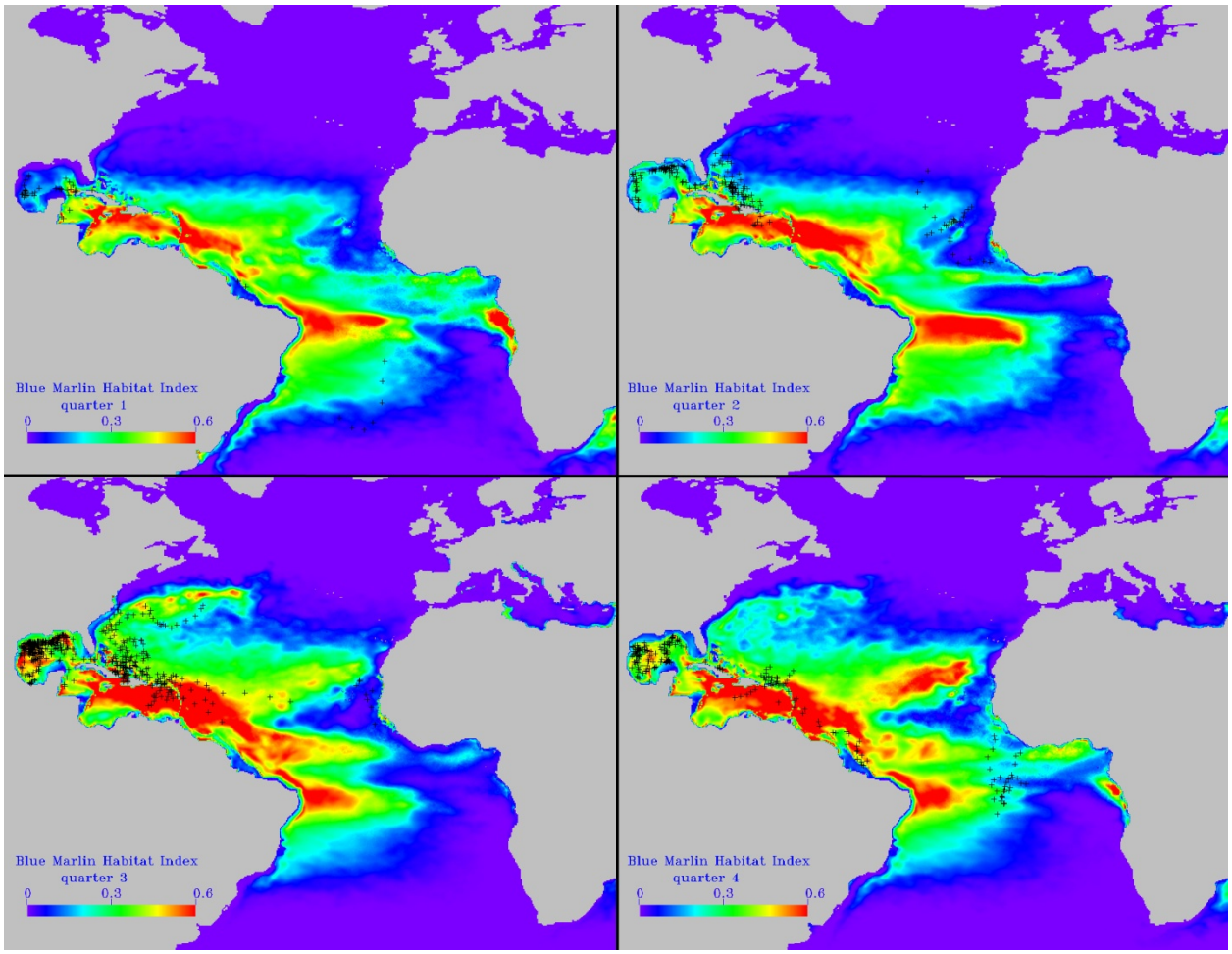

Figure 13. Seasonal average distribution of blue marlin feeding habitats from SEAPODYM model simulation of optimal feeding temperature T_a= 27.5 ^{o}C and DO threshold $\hat{O}$ =2.5 ml/L, over imposed with corresponding tag positions (black +).

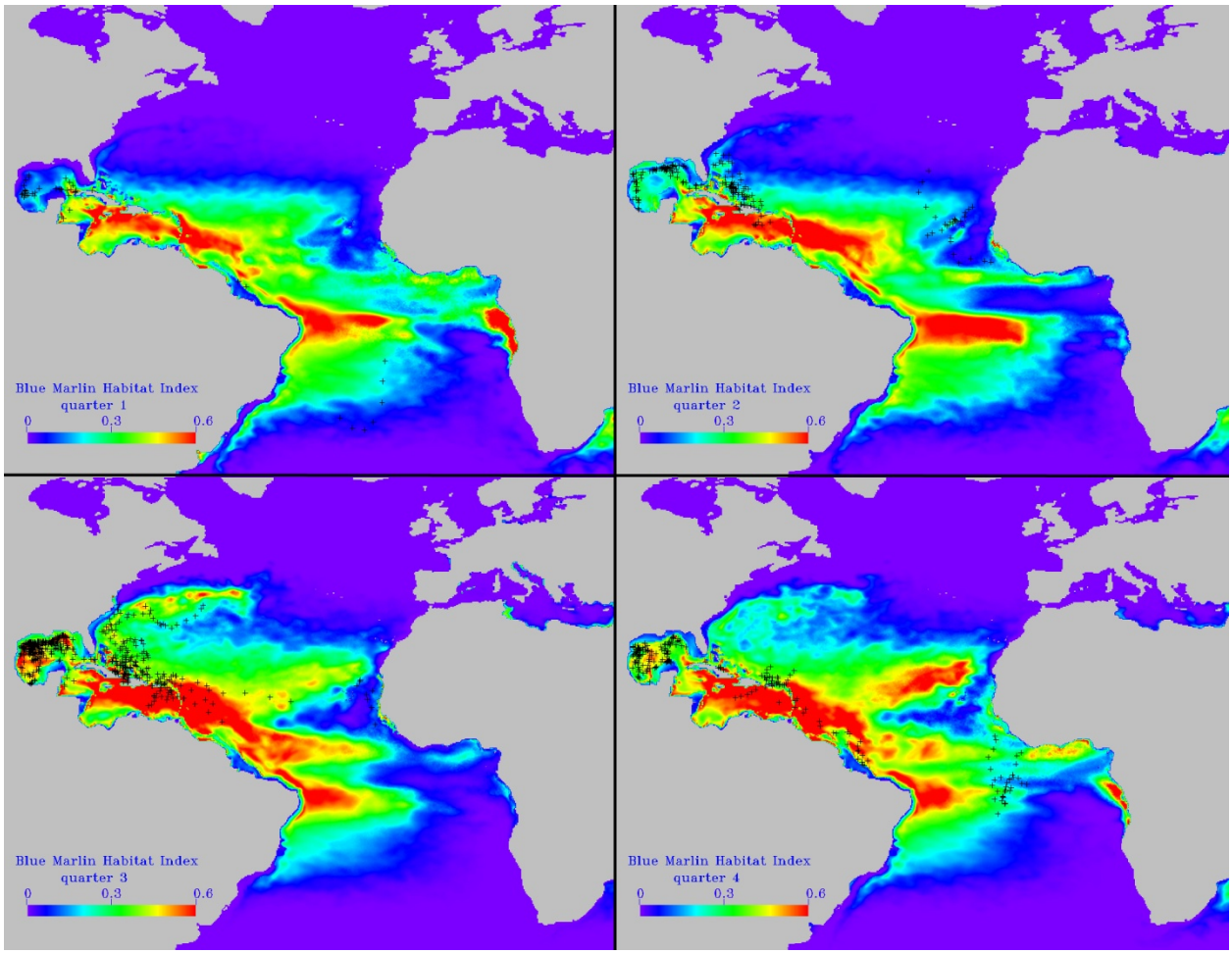

Figure 14. Areas (in 1000 km^2) of quarterly averaged feeding habitat indices as the function of optimal feeding temperature (T_a) at DO threshold $\hat{O}$ =4.5 ml/L from Seapodym model simulation runs for habitat quality level >0.5 (A) and level >0.1 (B).

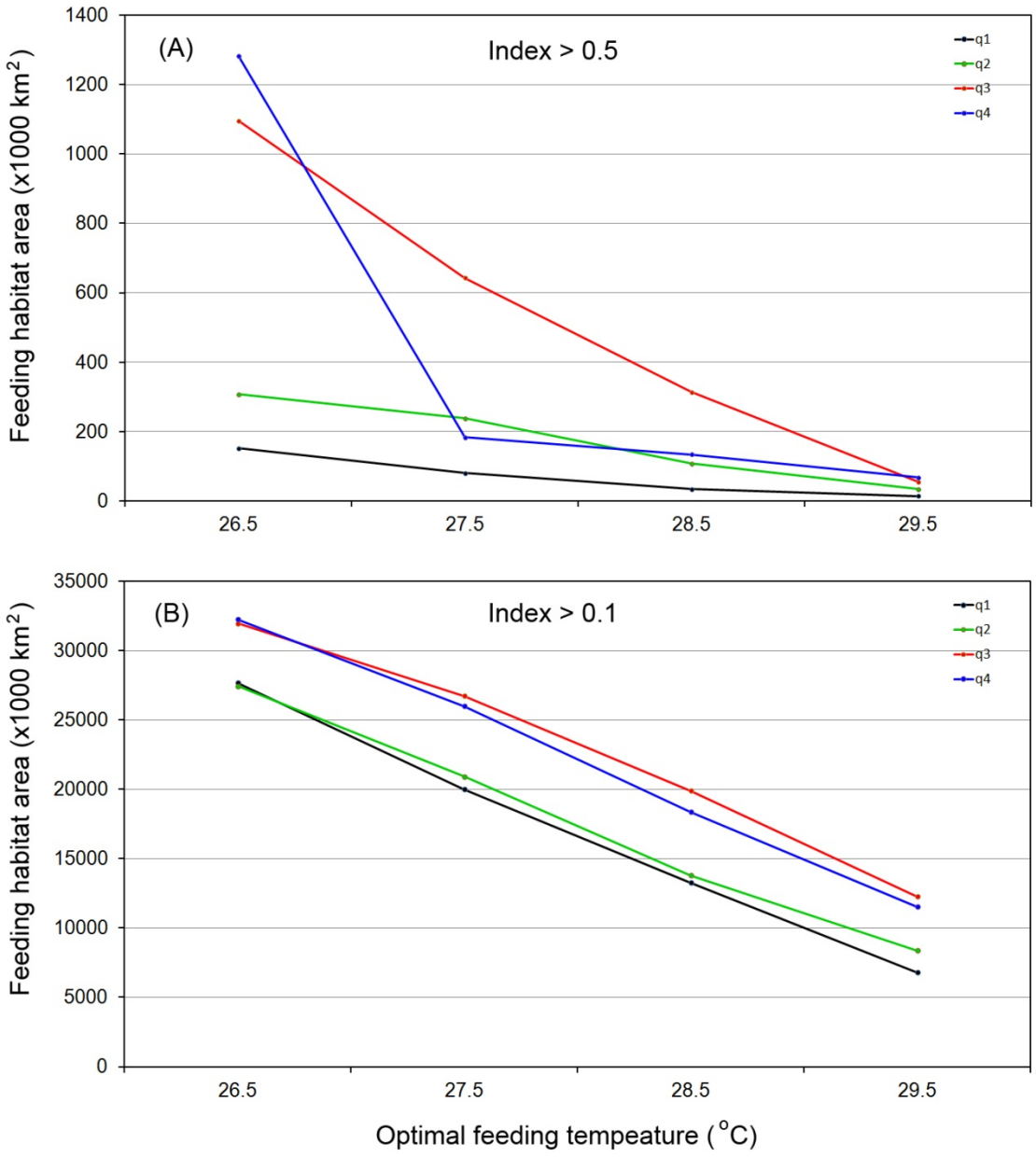

Figure 15. Areas (in 1000 km^2) of quarterly averaged feeding habitat indices as the function of DO threshold ($\hat{O}$) at the optimal feeding temperature (T_a = 27.5 ^{o}C) from Seapodym model simulation runs for habitat quality level >0.5 (A) and level >0.1 (B).

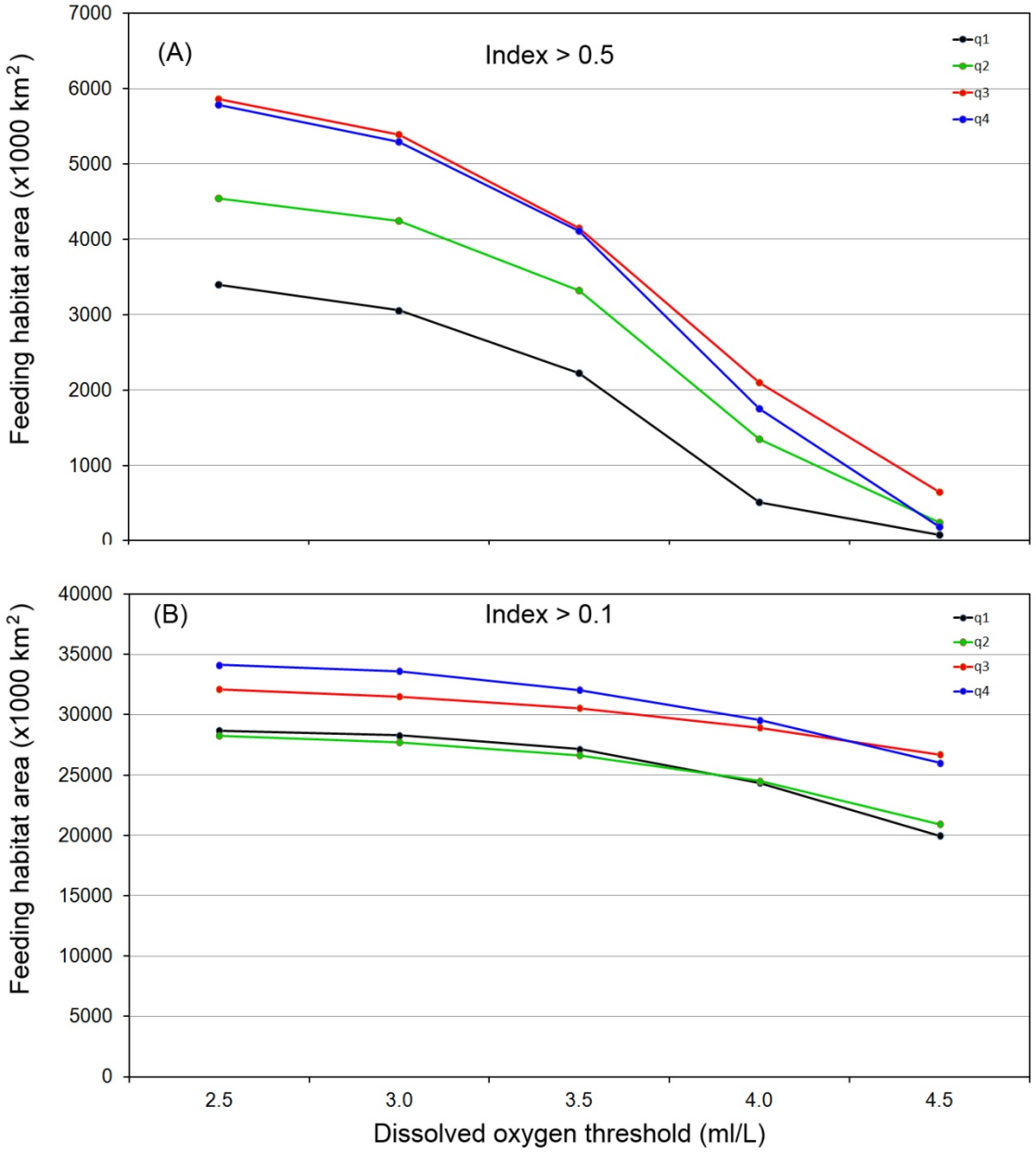

Figure 16. Seasonal average distribution of blue marlin spawning habitats from SEAPODYM model simulation of optimal spawning temperature T_0= 27.25 ^{o}C, over imposed with corresponding tag positions (black +).

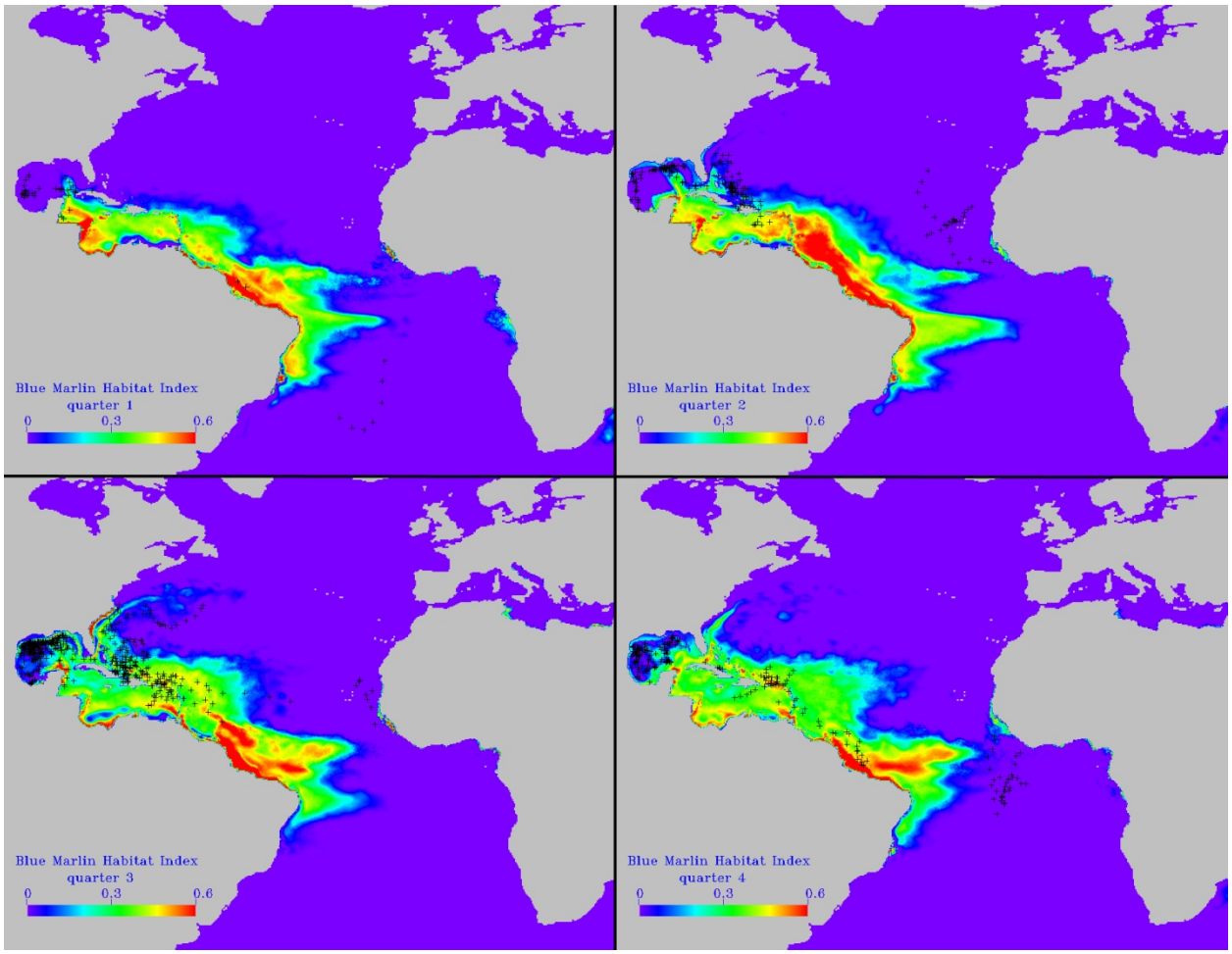

Figure 17. Seasonal average distribution of blue marlin spawning habitats from SEAPODYM model simulation of optimal spawning temperature T_0= 27.75 ^{o}C, over imposed with corresponding tag positions (black +).

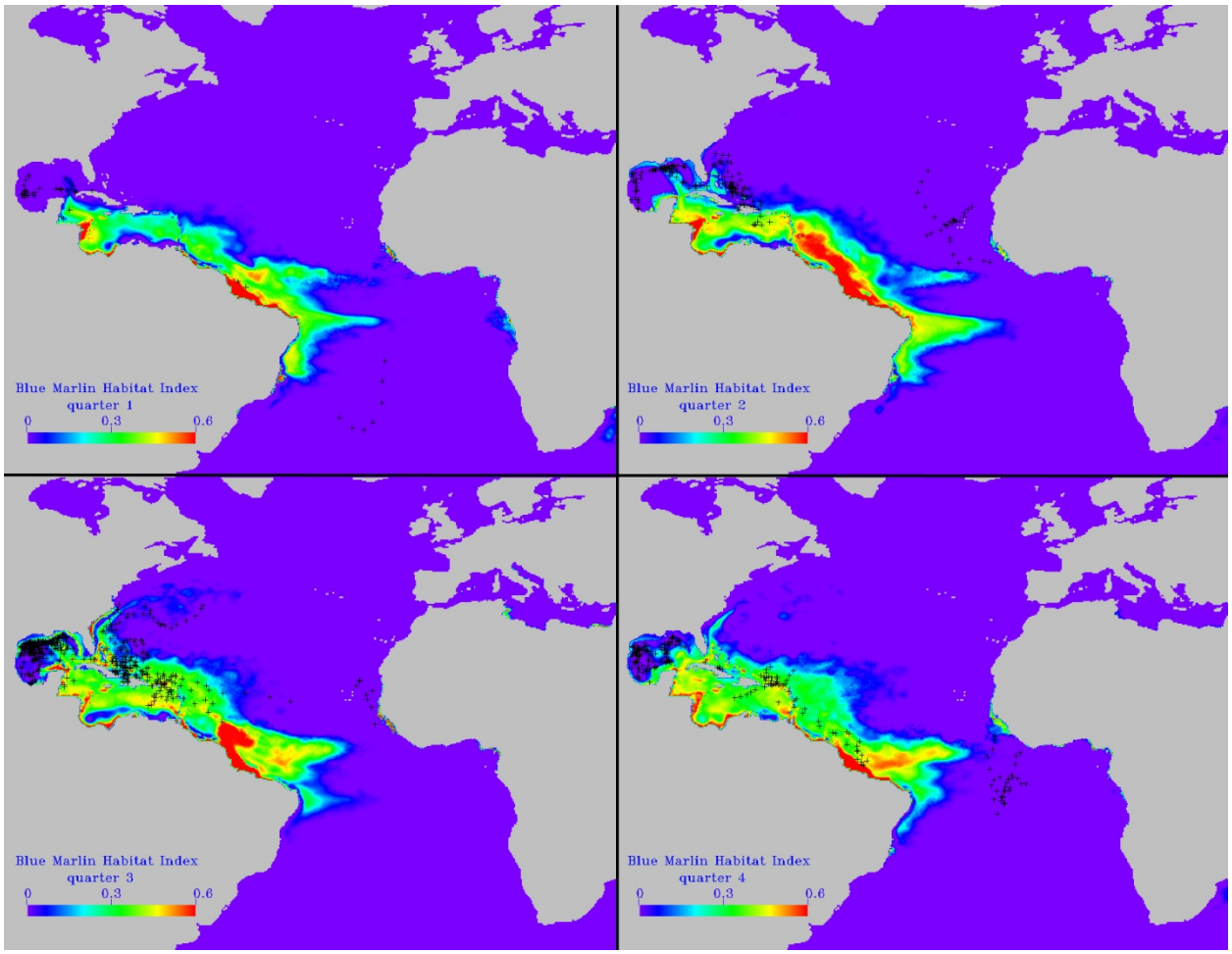

Figure 18. Seasonal average distribution of blue marlin spawning habitats from SEAPODYM model simulation of optimal spawning temperature T_0= 28.25 ^{o}C, over imposed with corresponding tag positions (black +).

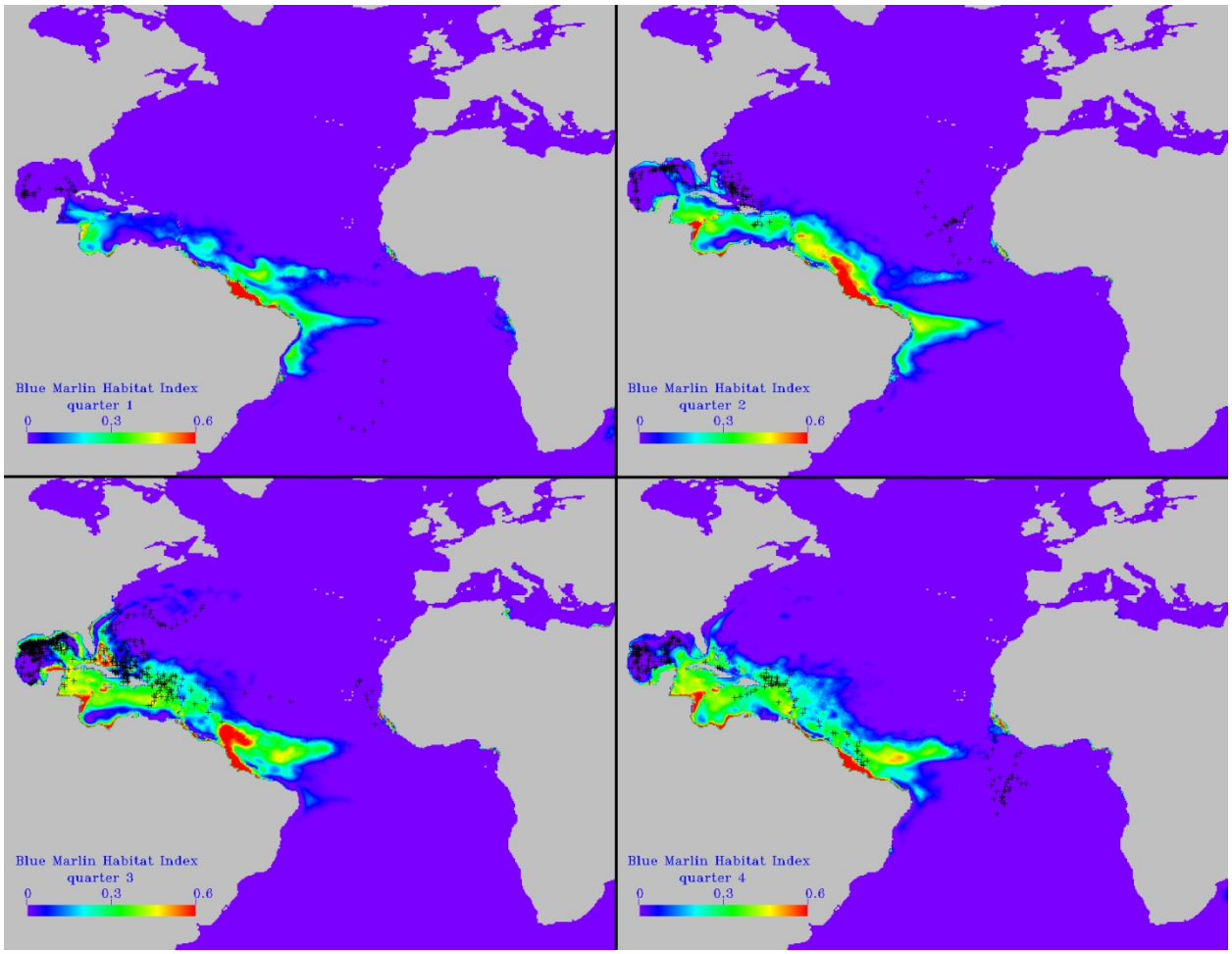

Figure 19. Seasonal average distribution of blue marlin spawning habitats from SEAPODYM model simulation of optimal spawning temperature T_0= 28.75 ^{o}C, over imposed with corresponding tag positions (black +).

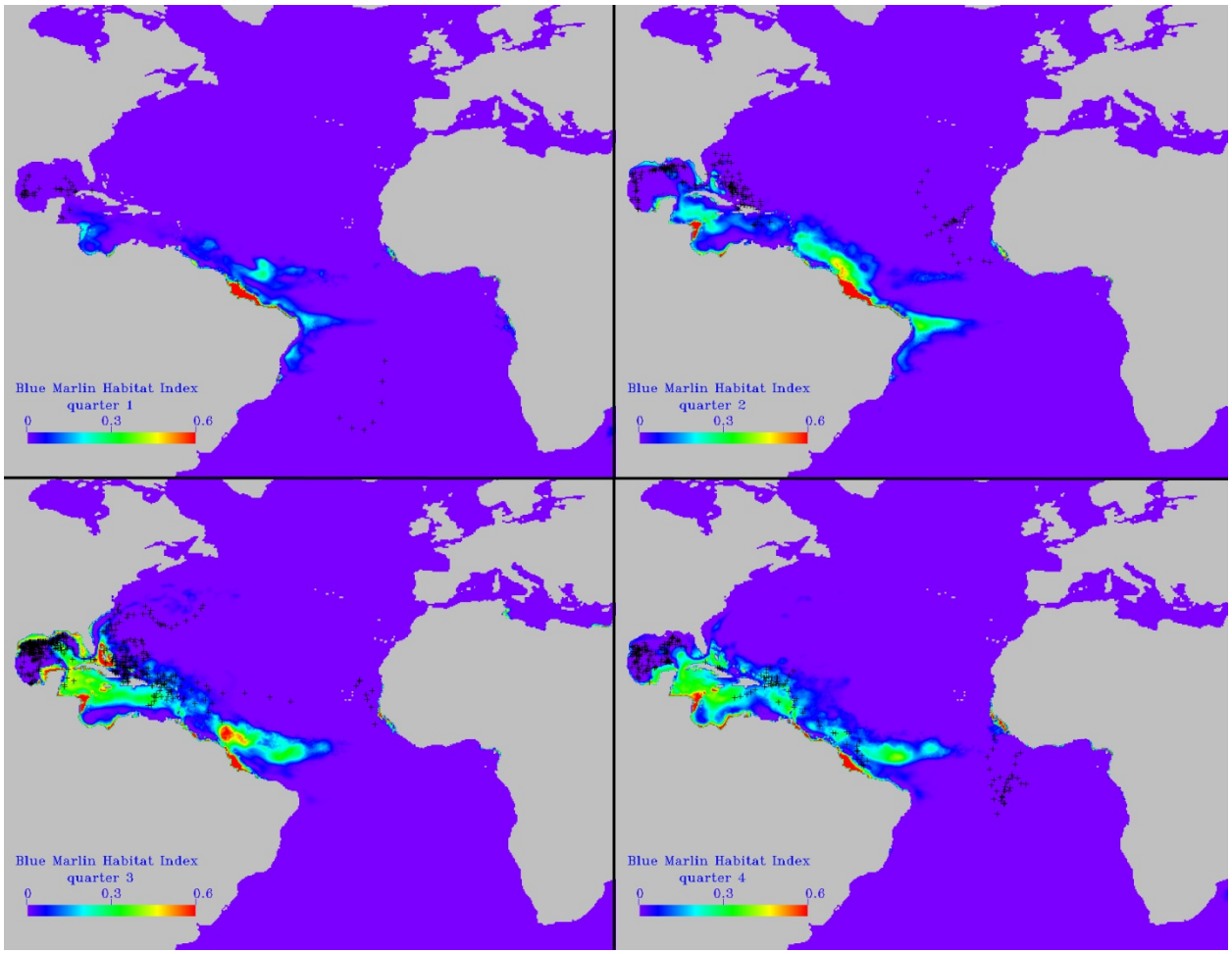

Figure 20. Areas (in 1000 km^2) of quarterly averaged feeding habitat indices as the function of optimal surface temperature (T_0) for blue marlin juvenile from Seapodym model simulation runs for habitat quality level >0.5 (A) and level >0.1 (B).

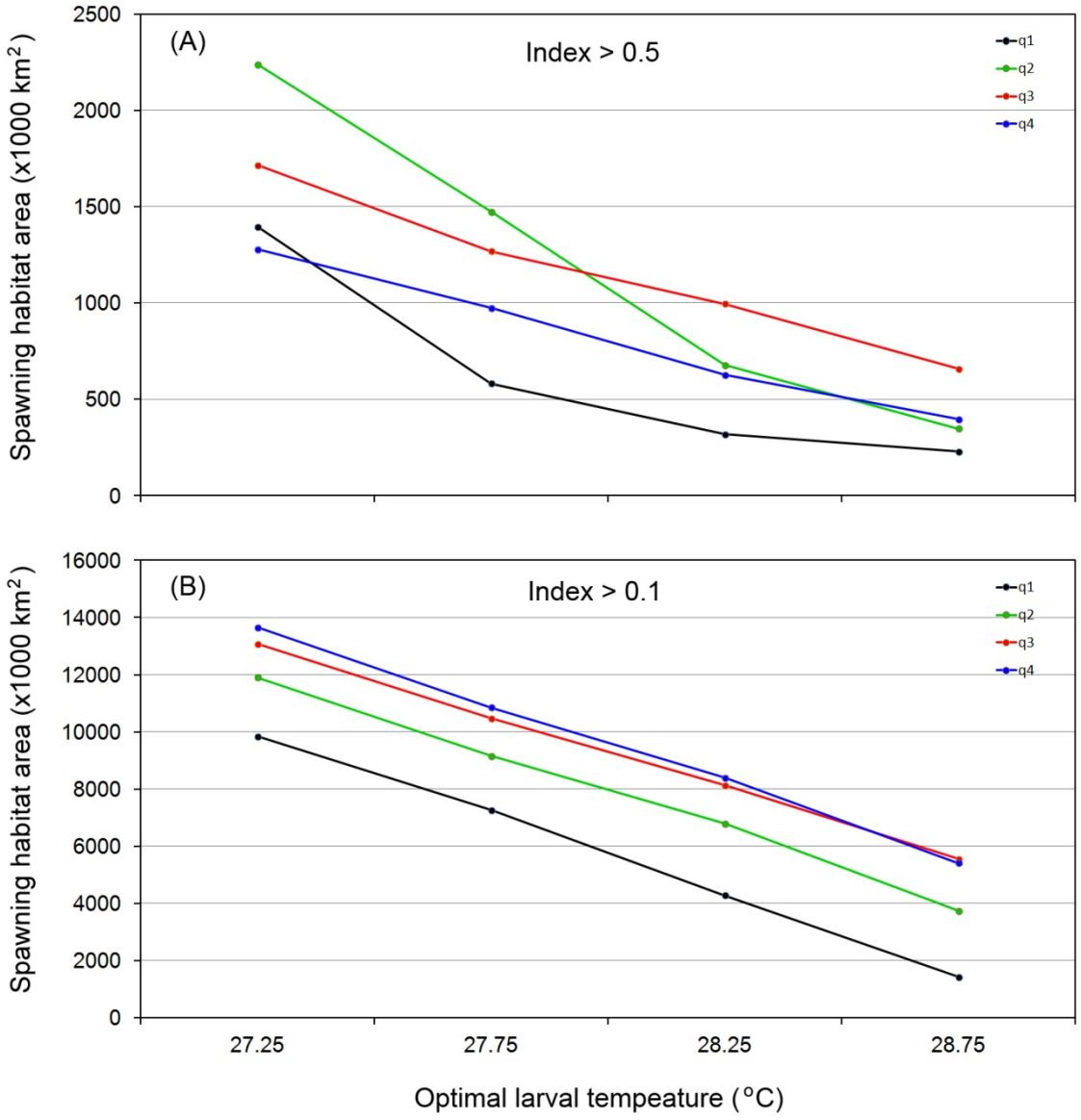

Figure 21. Map of dissolved oxygen concentration (ml/L) at 100 m depth (from World Ocean Atlas 2005) overlaying total blue marlin bycatch (yellow circles, in metric ton) of all countries in the Atlantic from 2000 to 2008. The white line is the 3.5 ml/L DO contour.

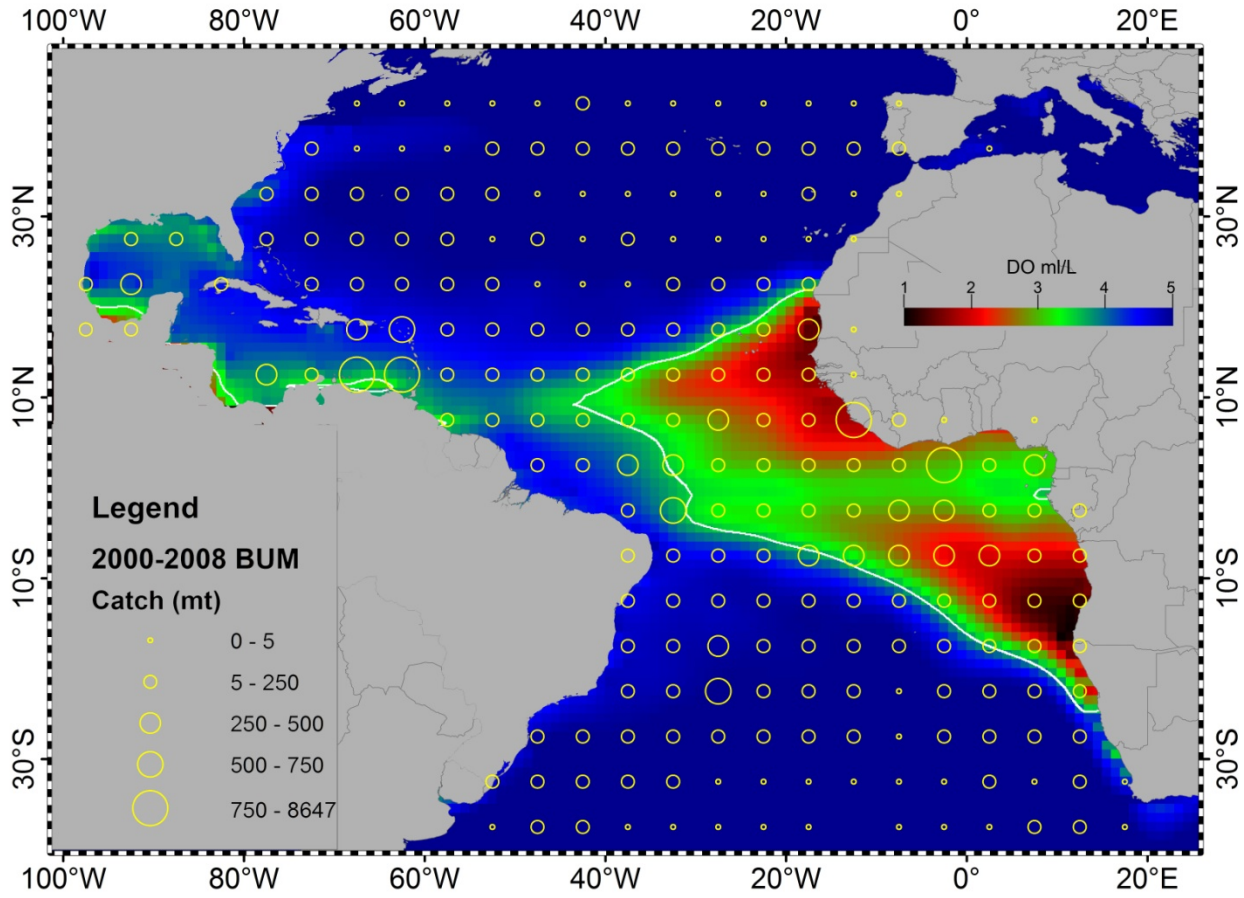

Figure 22. Map of dissolved oxygen concentration (ml/L) at 100 m depth (from World Ocean Atlas 2005) overlaying longline fishing efforts (million hooks, yellow circles) by most of countries in the Atlantic from 2000 to 2008. The white line is the 3.5 ml/L DO contour.

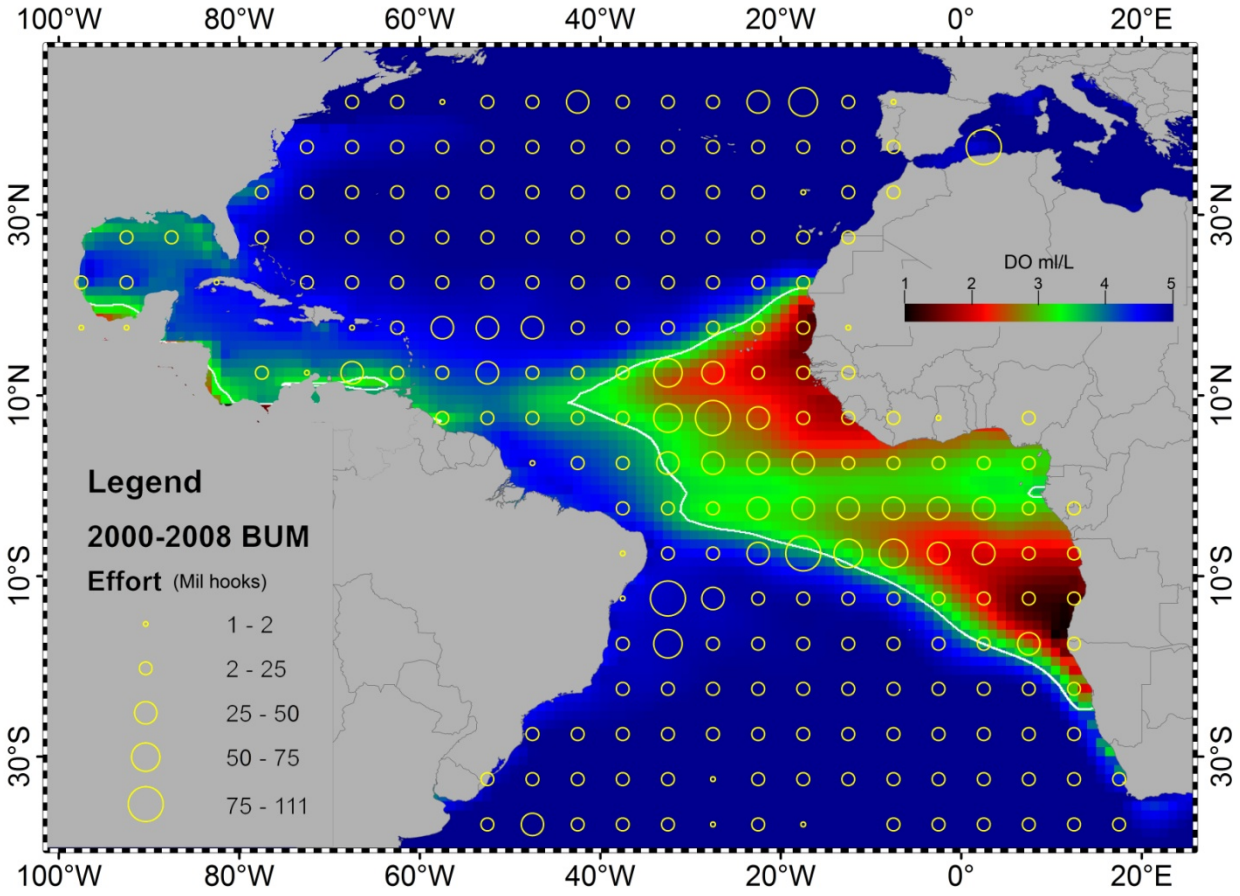

Figure 23. Map of dissolved oxygen concentration (ml/L) at 100 m depth (from World Ocean Atlas 2005) overlaying all country CPUE (mt/mil hooks, yellow circles) in the Atlantic from 2000 to 2008. The white line is the 3.5 ml/L DO contour.

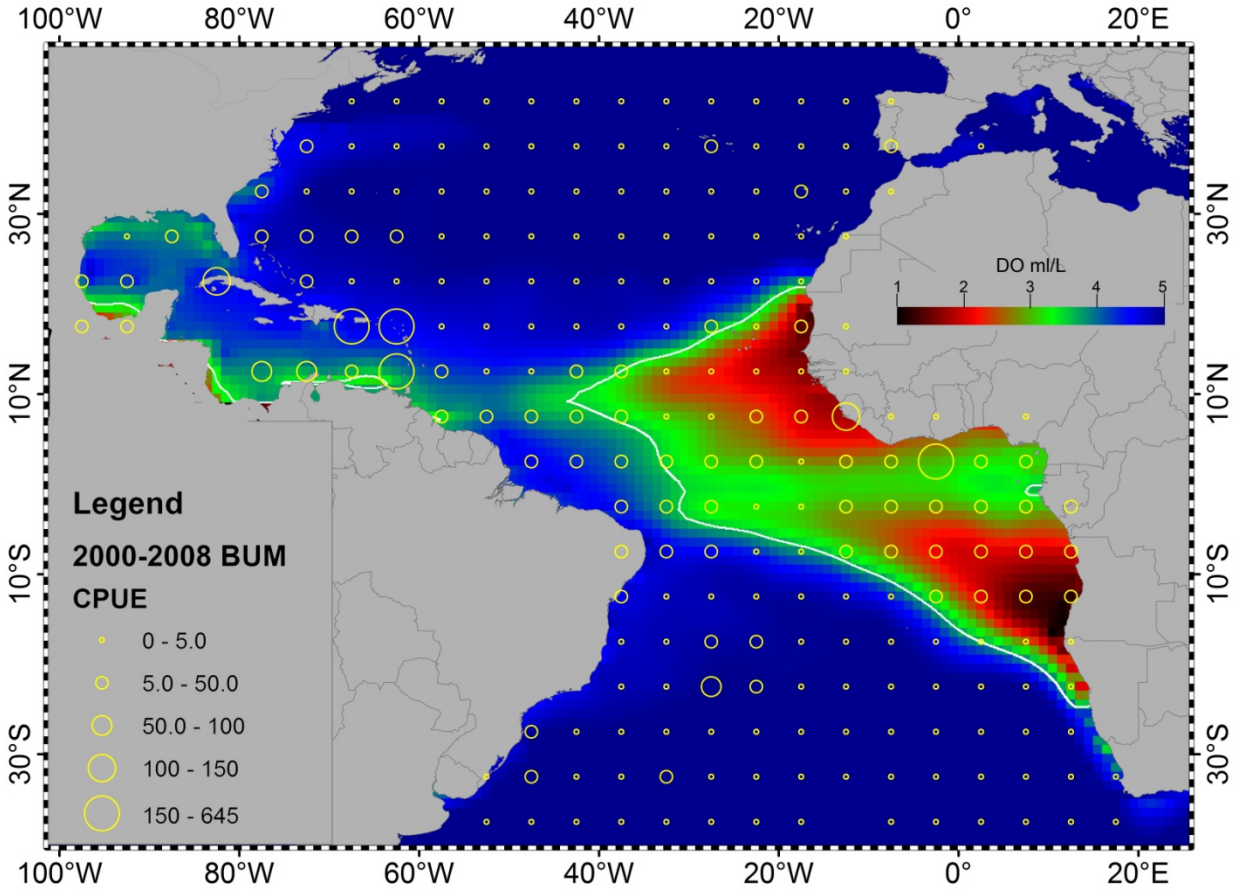

Figure 24. Seasonal average distribution of blue marlin bycatch CPUE (#/10000 hooks) by Japanese longline fishing fleet from 2000 to 2008.